AUSTRIAN MARSHALL PLAN FOUNDATION
VIENNA | AUSTRIA

Optimizing Peak Gust and Maximum Sustained Wind Speed Estimates for European Wind Storms Impacting Austria

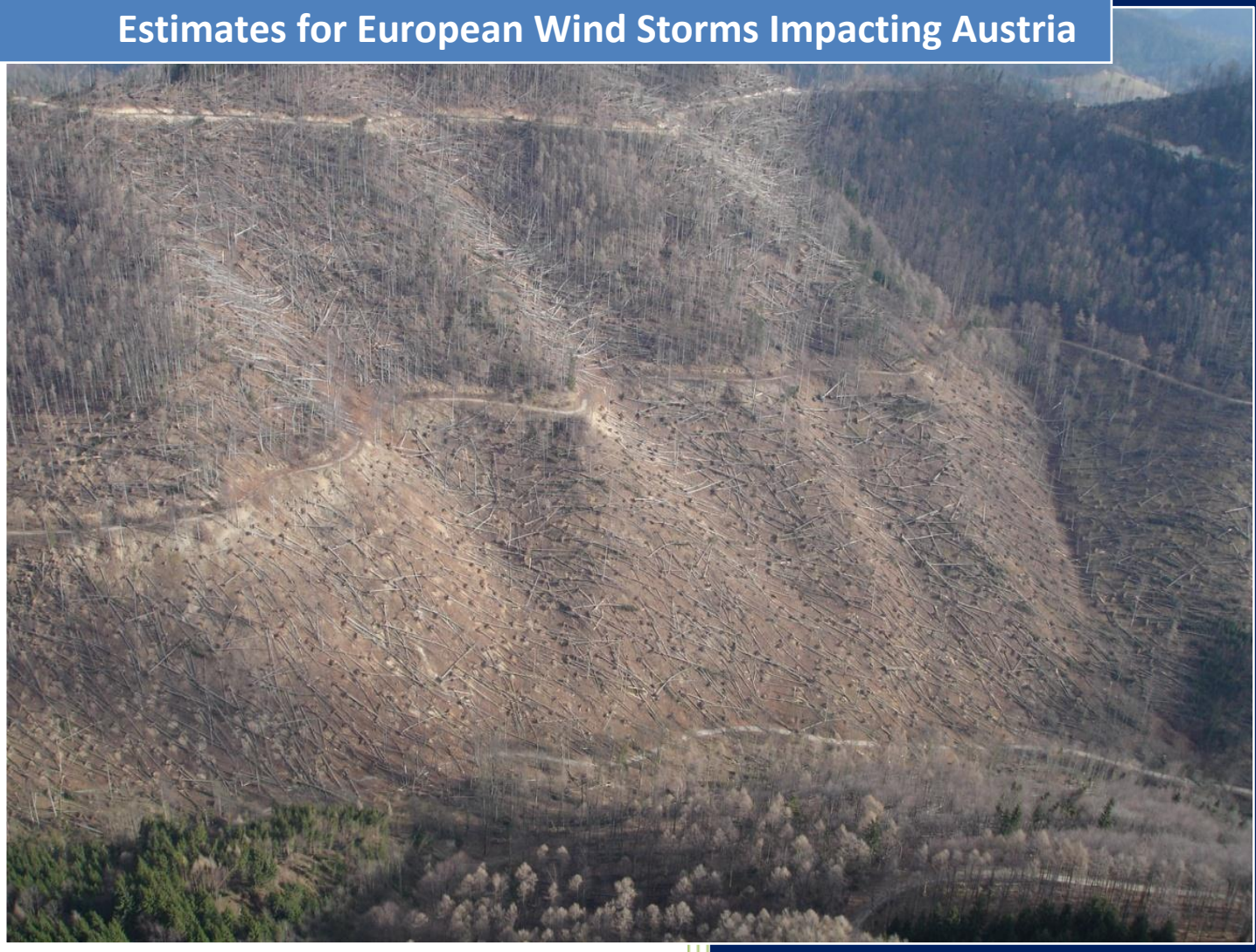

CARINTHIA UNIVERSITY OF APPLIED SCIENCES
FACHHOCHSCHULE KÄRNTEN

LSU

Timothy Andrew Joyner

Robert V. Rohli, Carol J. Friedland, Anna M. Treviño, Gernot Paulus

Table of Contents

Abstract

Wind storms result in significant damage and economic loss and are a major recurring threat to many countries. Multiple historic wind storms occurring over more than three decades across Europe have been analyzed previously to identify storm tracks, intensities, and areas of frequent high wind speeds. Maximum sustained winds and peak gusts were estimated based on an anisotropic (directionally-dependent) kriging interpolation methodology. Results suggest that coastal areas and mountainous areas experience the highest wind intensities during wind storms. These same areas also experience high variability over short distances and thus the highest error measurements associated with concurrent interpolated surfaces. For this reason, various covariates were utilized in conjunction with the cokriging interpolation technique to improve the interpolated wind surfaces for five wind storms that have impacted both the mountainous and topographically-varied Alps region and the coastal regions of Europe. The results show that use of cokriging improves our ability to interpolate surfaces for wind storms in mountainous and coastal regions. Land cover alone contributed to the highest reduction in station standard error in a majority of the models, while aspect and elevation (singularly and collectively) also reduced station standard error in most models as compared to the original kriging models. These advancements have the potential to improve damage estimate ratios for regions impacted by wind storms and will be used in a subsequent study to identify potential relationships between high winds and high damage in Austria.

Keywords: European wind storms, cokriging, land cover, aspect, elevation

1. Introduction

1.1 The physical and economic impact of wind storms

Mid-latitude cyclones produce wind storms across much of Europe predominantly during the winter months and are responsible for most of the destructive natural hazards in the region (Pinto et al. 2010). Much of the infrastructure-related destruction is attributable to extreme wind speeds that often impact multiple countries (Pinto et al. 2010). Certain climatic patterns such as the positive mode of the North Atlantic Oscillation (NAO) provide optimal conditions for cyclogenesis (Raible 2007). These patterns, along with other forcing mechanisms and climatic conditions, are in a constant state of flux with changes potentially attributable to anthropogenic-induced climate change (Handorf and Dethloff 2009), which has led many to suggest that changes in climate are at least partly to blame for recent surges in catastrophes (Schiermeier 2006). For this reason, predictions in loss estimates have been calculated under varying future climate scenarios to establish reinsurance rates based on storm intensity, or power, values (Leckebusch et al. 2007, Pinto et al. 2010) Increases in storm and concurrent wind intensity could lead to substantial increases in average annual damage across much of northwest Europe (Dorland et al. 1999).

Regardless of climatic changes, the impact from winter storms over the last several decades has been widespread across Europe and recent storms do not suggest a decrease in their frequency and intensity. Reports suggest that storms occurring in early 1990 and late 1999 resulted in large economic and insurance losses (Leckebusch et al. 2007). In central Europe alone, 56 percent of economic and 64 percent of insurance losses caused by natural hazards are due to these winter storms (Hofherr and Kunz 2010). Similar to hurricanes in the United States, European wind storms are named, but the names sometimes differ from country to country. Major storms normally follow the same nomenclature. The Lothar storm (December 25-27, 1999) is considered one of the most expensive storms in European history for insurance companies (Wernli et al. 2002, Leckebusch et al. 2007). Lothar was considerably stronger than other storms because of: (1) a stronger than normal upper-level jet, (2) rapid intensification of the storm resulting in an intensive vortex, and (3) higher than normal Atlantic sea surface temperatures (Wernli et al. 2002). Other similarly dangerous storms during this period were Kyrill (January 16-19, 2007) and Jeanette (October 26-28, 2002) (Heneka and Hofherr 2011).

Schmith et al. (1998) analyzed the trends in Northeast Atlantic winter storms (1875-1995) and found a gradual increase in the frequency of storms in the northeasternmost

portions of the storm track over the past 2 to 4 decades. Inter-annual and decadal influences were found to be the most dominant features in the temporal trends of these winter storms (Schmith et al. 1998). Leckebusch et al. (2007) used four global climate models to estimate storm damage in light of potential anthropogenic climate change (Leckebusch et al. 2007). Western Central Europe was found to be at a higher risk if adaptation to anthropogenic climate change was not considered. Donat et al. (2011) also modeled European winter storms and found northern portions of Central and Western Europe experienced increased wind speeds under future climate simulations. A decrease in extreme wind speeds was found in Southern Europe (Donat et al. 2011). Continued research on climatic variability and European winter storms is important because of the storms' impact on property losses in Europe, as they affect large areas, and are claimed to be "the most destructive natural hazards in Europe" (Klawa and Ulbrich 2003).

1.2 Review of wind storm data and related issues

There are some limitations to using station data to represent a wind field across a single storm. Klawa & Ulbrich (2003) stated that a single station can have its own individual climate, inferring the uncertainty that microclimatology may present when examining macroclimatological patterns. They present an economic loss model based on estimates of storm damage in Germany caused by high winds and concluded that a good estimate of insurance losses based upon peak gust measured at stations can be obtained. They also claimed that the Daria and Capella storms were very destructive for Germany, leading to 25 percent of all insurance damage claims during the period 1970-1997 (Klawa and Ulbrich 2003). Hofherr and Kunz (2010) emphasized the importance of high spatial resolution of station data to get an accurate evaluation of wind storm climatology and to find how local topographic features influence the wind field. Additionally, to better study the frequency of severe winter storms, longer data records are needed (Hofherr and Kunz 2010). Spatially, the strength of measured wind values is determined by a combination of local topography and large-scale atmospheric circulation variables. Hofherr and Kunz (2010) stated that large scale wind influences come from extratropical cyclones (their intensity and frequency), which are found to increase northward in Central Europe. At the local scale, orographic influences, land use, friction, and the boundary layer modify these synoptic winds. Gusts are most dependent on the roughness length of the terrain. Because of these local factors, the wind climatology of a station may vary considerably when compared to the synoptic-scale climatology (Hofherr and Kunz 2010). An attempt to calculate return periods of extreme winter storms (1957-

2002) was made by Della-Marta et al. (2009), and a need for longer station data was stressed. Schmith et al. (1998) claimed that testing for long-term trends using wind station data can be inaccurate due to changes in station location, observation methods, or instrumentation. Also, small trends that may be visible in records are best found when using long records, which are not always available at observation stations (Schmith et al. 1998).

Even though the use of station data has some limitations, it can be preferable to modeled estimates of data or radiosonde-based observations. Hofherr and Kunz (2010) discussed how wind data from stations are most popularly used in studies that evaluate hazards – both peak gust and mean wind speed values – due to the high level of accuracy on a local scale. The use of modeled wind data based upon upper-level air pressure is less accurate than actual readings from a meteorological station as they are not created using real wind data. Also the length of the record is not as long as station data, preventing any long-term studies. Radiosonde data, while it can be collected multiple times daily, only represent the atmosphere at a point. Station data can provide a better idea of fluctuations of wind at the local scale than many other data types and are highly appropriate for this study.

Estimation of peak gust values is necessary when peak gust data are missing. It is important to convert sustained wind speeds to a "probable maximum wind speed" over a shorter period because buildings and other structures are most affected by wind gusts of approximately 3 seconds in duration (Krayer and Marshall 1992). This is usually done by applying a "gust factor", which is "the ratio between the mean value of maxima and the mean value of a given effect associated with wind buffeting" (Solari 1993). Krayer and Marshall (1992) reviewed the Durst (1960) and Cook (1986) methods for calculating the gust factor and determined that the Durst method was most accurate in estimating peak gust wind speeds from mean wind speeds in tropical storms and hurricanes (Krayer and Marshall 1992). Solari et al. (1993) review various equations that have been used to calculate velocity of peak gusts, and found the various conversion values (V_1/V_{600} to V_5/V_{3600}) produced by other studies range from 1.07 to 1.68. These values vary largely based on the length of time used to calculate them. The Durst Curve conversion factor for data used in this study is 1.4299 (ASCE 7-10 2010).

1.3 Simulation of wind surfaces through interpolation of station data

There are many ways to simulate and interpolate wind surfaces. Spatial interpolation can produce both global/local and deterministic/stochastic estimates of unknown variables across a surface. These methods vary widely and it is important to understand the variable(s)

in question to select the most appropriate interpolation method (Luo et al. 2008). Deterministic methods do not use probability, meaning that all observed values are considered accurate (Luo et al. 2008). These methods are very common and include polynomial regression (PR), triangular irregular network (TIN), nearest neighbor (NN), splines, and inverse distance weighting (IDW). Stochastic methods, also known as geostatistical methods, use a probabilistic approach for data regularization and include artificial neural networks (ANNs), simulated annealing (SA), and various forms of kriging such as ordinary, universal, cokriging, multi-region, Bayesian, and neural network kriging (Lanza et al. 2001, Cellura et al. 2008, Zlatev et al. 2010).

Within the deterministic family, PR uses a linear regression approach to interpolate values between known or observed variables. PR is well-suited for fairly dense and compact areas, but it predicts poorly outside the range of the observed points (Akkala et al. 2010). The TIN approach creates triangles across a surface and the balance of mass between points is used to determine the unknown values. TIN produces a linear and coarse output. The NN approach assigns a value based on the value of the closest data point and is one of the simpler interpolation methods, but it is only considered accurate or suitable for a densely sampled surface (Akkala et al. 2010). Splining is a curvature method that still uses the exact observed values; however, the influence of the values decreases over distance, thus producing a two-dimensional curve as opposed to the linear surface produced by many other deterministic methods (Wahba 1981). Splining is considered one of the better deterministic methods of interpolation, but the smooth curves ignore trends and can hide uncertainty when data points are irregularly spaced (Luo et al. 2008, Akkala et al. 2010).

Stochastic interpolation methods are often more time-intensive and require a higher level of user input. ANNs can be applied independently of kriging and are used to reduce the over/under estimation of values through the use of a pivot station that "learns" the common correlation between the stations. This serves to decrease the oversmoothing that other interpolators cause by over-estimating low values and under-estimating high values, but ANNs can over-learn or under-learn a pattern (Akkala et al. 2010). For this reason, ANN's are best used in areas with high input variability over relatively short distances (Öztopal 2006). SA uses a linear regression function similar to the PR deterministic method to produce an interpolated surface, but a probability function is also applied to determine the distance from a point at which the relationship becomes insignificant (Sterk and Stein 1997). SA is best at capturing local variability, but the method is not well-suited to estimate large surface patterns (Sterk and Stein 1997).

Kriging interpolation methods are the most common stochastic techniques and they use probability and spatial correlation to create a surface that is weighted by observed values through a semi-variance function. Distance and direction are both utilized for the semi-variance function so it can account for anisotropic spatial patterns and trends in wind behavior (Luo et al. 2008). Since wind speeds often exhibit a direction in which they are increasing or decreasing across a surface, kriging methods are preferred over deterministic methods and other stochastic methods (Lanza et al. 2001, Luo et al. 2008, Akkala et al. 2010, Zlatev et al. 2010). However, microclimatological effects sometimes produce pockets or patches of high/low wind speed on a surface that can create confusion during kriging surface construction. The anisotropic function selects the dominant surface trend, but this trend may not align with the actual direction of wind speeds relative to a storm track, making it necessary to verify that the anisotropic azimuth direction reflects the direction of storm movement. During surface construction, kriging creates an unbiased surface where a polynomial function has not been forced to fit, thus eliminating edge and circular effects common in other interpolation methods (Akkala et al. 2010).

In a recent study by Luo et al. (2008), various forms of kriging performed better than other interpolation methods based on their mean error (ME) and root mean square error (RMSE). ME and RMSE accuracy metrics indicated that kriging produced an unbiased surface that was found to be ideal when modeling wind speed because values were not manipulated by a polynomial or linear fitting interpolation technique (Luo et al. 2008). ME and RMSE are commonly used evaluation metrics when determining the quality and reliability of interpolation techniques because they provide a good means of comparing across various time periods and between various methods. Kriging consistently outperformed deterministic methods such as IDW, which not only received poorer ME and RMSE scores, but also produced a surface with an illogical "bullseye" effect centered on each weather station (Luo et al. 2008).

When used for wind speeds, kriging is considered an approximate predictor because of the incorporation of a nugget effect – a variation that exists at shorter distances than the distance between sample points. If the nugget size is greater than zero, then there is a nugget effect. The nugget size is used during the kriging process to represent independent error and it is the intersection of the data with the y-axis. For example, the correlation between observed wind speed values is plotted on a 1x1 variable diagram as the first step in creating a semivariogram model. The gap between the origin and where the semivariogram begins is referred to as the nugget size (Figure 1 represents a hypothetical example). The plot

illustrates the correlation that surrounding values have at varying distances. Once the correlation diminishes to an insignificant amount, then the "sill" is reached, indicating that the values no longer have spatial dependence. The distance between the nugget size and the sill is called the range and all of these values are used concurrently to create the semivariogram for kriging. Range, sill, and nugget size determine at what distance the wind speed levels off or changes. For example, wind speed may decrease rapidly over land when the wind direction is from the north, but wind speed may decrease less rapidly over land when the wind direction is from the west. This could be caused by a variety of land surface factors (often topography and surface roughness), but anisotropic semivariograms account for wind direction and distance by examining the sill in each direction when making probabilistic surface estimates.

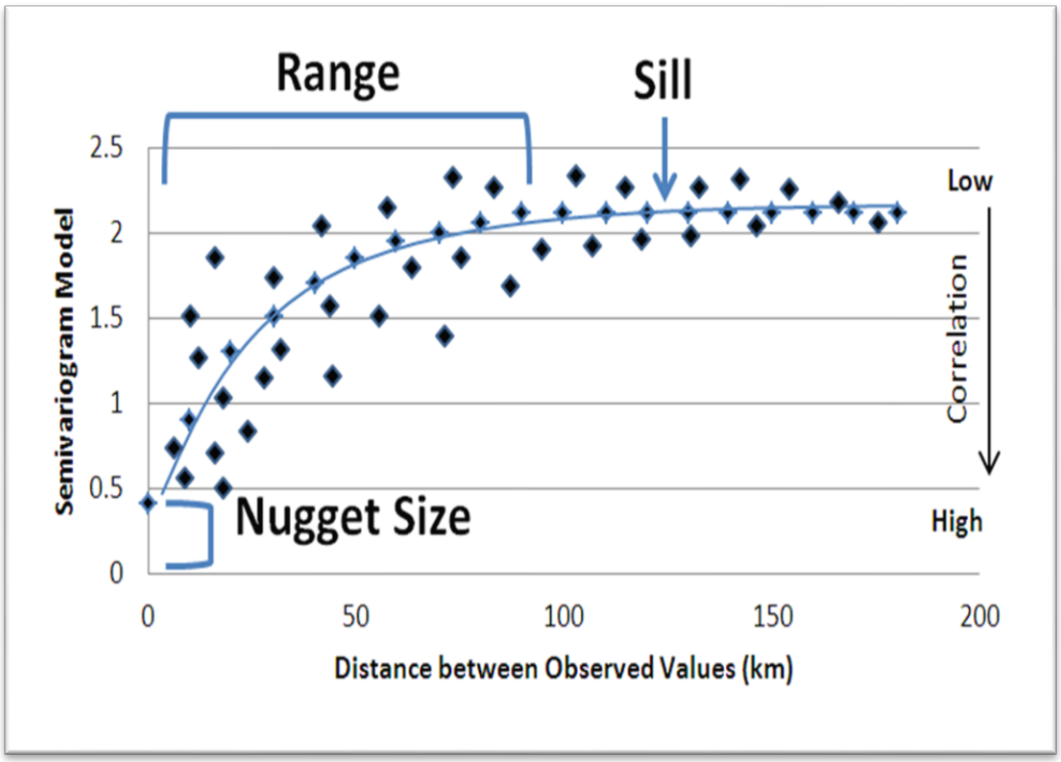

Figure 1. Nugget size represents where the data and the y-axis intersect. Range is the distance from an observed value at which spatial dependence exists (between the nugget and sill). The sill is the upper limit where spatial dependence ceases to exist, or where influence ends.

Ordinary and universal kriging are the two most common forms of kriging. Ordinary kriging assumes an unknown constant trend and utilizes the points within a specified search radius for semivariogram creation, while universal kriging assumes a general linear mean value trend across an entire study area (Cressie 1986, Cressie 1990). Cokriging uses an additional variable or variables sampled from the same location (e.g., elevation) to make an

assisted estimation (Helterbrand and Cressie 1994). A spatial correlation is determined between the main variable and covariable(s) and the relationship is modeled. Cokriging is ideal for interpolating wind surfaces when stations are well distributed across a proportionate surface in a study area (i.e., if 10 percent of a study area is mountainous, then 10 percent of the wind stations should be located in the mountainous region) (Luo et al. 2008). However, knowledge-assisted forms of kriging such as cokriging are time-intensive and often require land segmentation and *in situ* verification, making cokriging an illogical choice for large datasets where this information is not available. Bayesian forms of kriging are the most computationally intensive with Monte Carlo or Markov chain techniques used to minimize the amount that uncertainty impacts model parameters (Lanza et al. 2001). There is currently no precedent for using the Bayesian approach for wind surface interpolation. ANNs have also been coupled with various kriging methods, but similar problems that occur with ANNs used outside of the kriging framework also occur when coupled with kriging (Cellura et al. 2008). Table 1 provides examples of studies investigating the interpolation of wind speeds and other climatic data and highlights the methods that were recommended by each study. The literature does not recommend that deterministic methods be used for wind surface interpolation and the overall trend suggests that kriging (in various forms) continues to be a very good method for interpolating wind surfaces, but other network- and knowledge-based adaptations or improvements to kriging are ongoing. Many kriging adaptations are very promising, but a consensus has yet to be reached on a clear adaptation that will supersede current kriging methodologies. Further, the majority of these advanced studies focused on local- to regional-scale wind surfaces within a single country and not large-scale surfaces that would include multiple countries. It is very difficult and time-intensive to apply advanced network- and knowledge-assisted kriging adaptations across multiple countries or an entire continent without more detailed information about stations, microtopography, local environment, and other geographic features. The widely-varying terrain of Europe presents a challenge to these advanced approaches. As new data become available and as these new methods are explored and improved in the coming years, they may prove more useful for large-scale analyses and potentially be included in future software packages (e.g., ArcGIS).

Table 1. Interpolation studies that examined wind variables.

Source	Study Area(s)	Event Type	Methods Examined	Methods Recommended
(Bentamy et al. 1996)	Tropical Atlantic Ocean	Avg. wind speed (multi-year)	Kriging	Kriging
(Sterk and Stein 1997)	Sahelian zone (Niger)	Wind-blown mass transport from 4 storms (1993)	Linear Interpolation (Simulated Annealing), Ordinary Kriging	Ordinary Kriging was best at predicting unsampled locations; Simulated Annealing was best for local variability
(Phillips et al. 1997)	Southeast US	Ozone exposure (multi-year; used wind direction)	Inverse Distance Weighting, Inverse Distance Squared Weighting, Ordinary Kriging, Cokriging	Cokriging and Ordinary Kriging
(Venäläinen and Heikinheimo 2002)	Finland	Daily wind speed, temperature, humidity, precipitation, radiation	Kriging	Kriging
(Öztopal 2006)	Marmara, Turkey	Daily wind speed over time (potential wind energy)	Artificial Neural Network	Artificial Neural Network
(Cellura et al. 2008)	Sicily, Italy	Avg. wind speed at 50m for wind farm (multi-year)	Neural Network, Radial Basis Functions, Neural Kriging, Ordinary/Univeral Kriging, Inverse Distance Weighting,	Coupled Neural Network/Kriging Interpolators
(Luo et al. 2008)	England, Wales	Avg. wind speed (Mar. 27, 2001)	Trend Surface Analysis, Inverse Distance Weighting, Local Polynomial, Thin Plate Spline, Kriging, Cokriging	Cokriging and Ordinary Kriging
(Zlatev et al. 2009)	United Kingdom	Avg. wind speed/direction	Ordinary Kriging	Ordinary Kriging
(Zlatev et al. 2010)	United Kingdom	Avg. wind speed (Mar. 27, 2001)	Ordinary Kriging, Universal Kriging, Cokriging, Multi-region Ordinary Kriging	Multi-region Ordinary Kriging (Knowledge-assisted)
(Akkala et al. 2010)	None (Review article)	Multiple meteorological events (including wind storms)	Nearest Neighbor, Triangular Irregular Network, Polynomial Regression, Polynomial Interpolation, Trend Surface Analysis, Inverse Distance Weighting, Splines, Kriging, Radial Basis Functions, Artificial Neural Networks	Knowledge based/assisted techniques

1.4 Cokriging

While ordinary kriging is a common and often-used interpolation method, cokriging is less popular because of the added complexity involved in selecting appropriate covariates.

Odeh et al. (1995) utilized various forms of cokriging along with ordinary kriging, universal kriging, multi-linear regression, and regression kriging models to predict soil properties based on landform attributes. The study revealed that the cokriging models were superior to ordinary kriging models because they accounted for the covariation between the predictor variable (soil properties) and specific terrain attributes (slope angle, aspect, plan curvature, and profile curvature). An earlier study examining soil physics concluded that cokriging reduced the estimation variance and improved estimates of under-sampled variables by accounting for the spatial correlation between available water content, water stored at 1/3 bar, and sand content values (Vauclin et al. 1983). Additionally, remotely sensed data were utilized to predict soil organic matter (Wu et al. 2009) and for resolution improvement (Atkinson et al. 2008, Pardo-Iguzquiza et al. 2011). Spatial resolution of remotely sensed (satellite) images was improved in one study based on the inter- and intra-correlation between images utilizing a moving window approach (Pardo-Iguzquiza et al. 2011) and in a separate study based on a point-support network (Atkinson et al. 2008). Air pollution surfaces have also been improved through the cokriging process. To reconstruct air pollution maps the results of a Chemical Transport Model simulation was used as the covariate, while ozone concentrations and daily mean particulate matter (>10) concentrations were the predictor variables (Singh et al. 2011). Generalized additive models were used to produce global residuals near nitrogen dioxide and nitrogen oxide sampling locations in Southern California and the predicted oxide surfaces greatly improved with very high cross-validated R^2 values (~0.9) (Li et al. 2012).

Cokriging has been used to improve temperature and precipitation interpolated surface estimates. Aznar et al. (2012) applied cokriging to produce a time series of monthly mean temperatures in Northeastern Canada between 1961-2000. Temperature recordings from 202 meteorological stations were utilized as the predictor variable and regional climate model-derived temperatures were incorporated as a covariate because of their incorporation of local variance (Aznar et al. 2012). This study resulted in accurate and publicly available monthly mean temperature grids for the region. Mahdian et al. (2009) utilized multiple geostatistical techniques to estimate monthly and annual temperature and found that cokriging with elevation used as a covariate produced a surface with a low mean absolute error compared to most of the other models.

Cokriging has also been proven to be an optimal method for estimating precipitation surfaces based on the use of various covariates (Wenxia et al. 2010, Luo et al. 2011, Wang et al. 2011). Topography, or elevation, was especially effective for cokriging models that

examined the Taihu Lake Basin in China (Luo et al. 2011) and the Chongqing tobacco planting region of China (Wang et al. 2011) in areas where topography varied greatly. Improvements compared with other models were negligible in areas of homogenous topography. Wenxia et al. (2010) expanded on the traditional covariate of elevation by also including geographic factors (longitude, latitude, terrain, slope, aspect, and shelter degree). Collectively, cokriging models utilizing both topographic and geographic variables outperformed the IDW method and the cokriging method that incorporated only elevation.

On occasion, multiple climatic (average daily maximum temperature, wind direction frequencies) and non-climatic (nitrous oxide emissions, distance downwind from nitrous oxide emission sources) variables have been used to estimate a surface – ozone exposure in the case of Phillips et al. (1997). The use of wind direction by Phillips et al. (1997) alludes to the ability of kriging and cokriging to account for anisotropy within the model. In addition to the inherent ability to account for anisotropy, cokriging of wind speed adds the ability to incorporate many of the covariates (e.g., topography, aspect, terrain, slope, etc.) used in previous studies. Luo et al. (2008) examined seven different methods of spatial interpolation and concluded that cokriging with elevation as a covariate produced a superior daily mean wind speed surface with better accuracy metrics than the other six surfaces (one of which included ordinary kriging). Similarly, Zlatev et al. (2010) also found cokriging to be superior to other forms of kriging and spatial interpolation based on lower error measurements when estimating daily mean wind speed. In both studies, error reduction occurred over a rugged landscape (United Kingdom) indicating that the use of elevation aided in model improvement. A separate study in Poland confirmed the impact of elevation on improving wind surface estimates when applied to a topographically diverse landscape (Sliz-Szkliniarz and Vogt 2011). Since Poland is a very flat country in most areas, cokriging (with elevation) showed little to no improvement over the ordinary kriging approach, which would be expected in a topographically homogenous region. The results of Luo et al. (2008), Zlatev et al. (2010), and Sliz-Szkliniarz and Vogt (2011) provide substantial evidence that covariates can help improve wind surface estimates in topographically varied regions, while maintaining the previous accuracy of ordinary kriging surface estimates in more topographically homogenous regions. Additionally, spatial distribution and density are important when modeling and mapping data (MacEachren and Davidson 1987) and the flexibility and robustness of cokriging, and geostatistical methods in general, account for variance in station distribution and density thus indicating that they are well-suited for wind observation data (Sliz-Szkliniarz and Vogt 2011).

1.5 Study area and objectives

Accurate and reasonable wind surface estimates that capture regional wind speeds and directions can be created for large areas of Europe using an anisotropic semivariogram-derived kriging methodology (Joyner et al. *in review*). Surface wind estimates suggested that coastal and mountainous regions often experienced the most extreme wind speeds. Inland Europe, specifically the Black Forest and northern Alps, displayed very high wind speeds relative to the surrounding areas – indicative of a complex topography/wind interaction. Coastal and mountainous weather stations experienced the most intra-storm wind speed variability and also reported some of the highest error measurements – most likely a result of landscape heterogeneity and post-model smoothing. Because of these high error measurements, this study will examine multiple covariates through the cokriging technique in an effort to create more accurate surface wind interpolations and to improve understanding of local wind variability in these environments. Previous studies that identified cokriging as superior for estimating surface winds only utilized elevation as a singular covariate (e.g., Luo et al. 2008, Sliz-Szkliniarz and Vogt 2011); this study will also utilize aspect and land cover in addition to elevation. The research questions for this study are as follows:

1) To what extent does cokriging improve interpolated wind surfaces in the coastal and mountainous regions of Europe, compared to ordinary kriging methods?

2) Which covariate(s), if any, is(are) most influential in improving wind surface interpolations in diverse terrain?

2. Data and Methods

2.1 Wind storm and covariate data and adjustments

Five wind storms occurring between 1999 and 2008 were selected for this study out of the total of 18 that were available for Europe (Table 2). These storms were selected based on a combination of factors including extent and degree of impact and intensity as well as the availability of supporting data about each storm. Each of the five storms impacted both coastal and mountainous regions where standard errors were highest, thus increasing the potential to show improvement in predicting surface winds in these areas through utilization of the cokriging methodology.

Table 2. European wind storms and impacted countries.

Year	Date	Popular Name	Countries
1999	25-27 December	Lothar	France, Switzerland, Germany
2002	26-28 October	Jeanette	UK, Denmark, Sweden, Germany, Netherlands, France, Austria, Poland, Czech Republic, Belgium, Ireland
2007	16-19 January	Kyrill	France, Netherlands, Germany, UK, Belgium, Austria, Ireland
2008	24-26 January	Paula	Poland, Germany, Austria, Denmark, Norway, Sweden
2008	29 February-2 March	Emma	Germany, Austria, Czech Republic, Belgium, Netherlands, Switzerland, Poland

Wind data for this project were obtained from the World Meteorological Organization (WMO) observation stations sourced through a third party provider. The WMO Standard (World Meterological Organization 2008) for measuring sustained wind is an average of values obtained for the 10 minutes previous to the observation time. The WMO Standard for measuring peak gust is a continuous average of values over a 3 second period. Wind instruments according to WMO standards are to be located at a height of 10 m in open terrain, and wind data are adjusted for local topographic effects through the use of an exposure correction factor. For example, a station located at the top of a hill would have a correction factor applied to the data to account for the changes in wind speed caused by the hill. According to the WMO chapter of wind standards (World Meterological Organization 2008), the wind speed would be more representative of the region rather than the individual hill. When a station that records wind speeds is not located at a 10-m height, the station data are to be adjusted to a 10-m estimated speed using a logarithmic wind profile. A preliminary quality control analysis of the European wind storm data was conducted by plotting the sustained and peak gust values against the mean of each variable. Outliers were examined to determine whether the values were reasonable for the given atmospheric conditions. Stations that were modeled most successfully came proportionately from those with 10-m measurements and those at which the 10-m wind was adjusted from measurements at a different height. Based on this analysis, it appears that the model performance is not unduly biased by the vertical adjustment of station-based wind values.

A set of 5 storms was analyzed over the period 1999-2008 for Europe (Table 3). These storms occurred mainly during cool-season months (October through March). The MATLAB® statistical computing program was used to extract sustained wind and peak gust values from the original data files. The maximum daily value was extracted at each station for sustained wind and peak gust and the station maxima were identified from the daily maxima. A storm summary showing the statistics of data provided for sustained wind (Table

4) and peak gusts (Table 5) was produced for each storm. The sustained wind data were fairly consistent between the storms, with only 0.6 percent of the data values missing and an overall mean sustained wind value of 14.2 meters per second (m/s). Peak gust measurements were missing for 77.3 percent of the hourly observations and the overall mean peak gust was 25.3 m/s. Lothar had the greatest mean sustained wind at 16.4 m/s and Emma had the largest mean peak gust at 27.1 m/s. Paula had the lowest mean sustained wind at 10.9 m/s and also the lowest mean peak gust at 21.0 m/s.

Table 3. Number of stations reporting data.

Year	Storm	Sustained	Peak Gust	Sustained & Peak Gust	Total
1999	Lothar	321	202	202	322
2002	Jeanette	1014	406	406	1016
2007	Kyrill	637	418	418	637
2008	Paula	662	130	130	663
2008	Emma	495	216	216	496

Table 4. Sustained wind storm summary table (m/s).

Year	Storm	Mean	Median	Minimum	Maximum	Range	Percent Missing
1999	Lothar	16.4	15.9	0.0	40.1	40.1	1.4%
2002	Jeanette	13.9	13.4	0.0	42.0	42.0	0.5%
2007	Kyrill	15.8	16.4	1.0	36.8	35.8	0.7%
2008	Paula	10.9	10.0	0.0	42.0	42.0	0.5%
2008	Emma	13.9	14.0	0.0	47.0	47.0	0.1%
	Average	14.2	13.9	0.2	41.6	41.4	0.6%

Table 5. Peak gust storm summary table (m/s).

Year	Storm	Mean	Median	Minimum	Maximum	Range	Percent Missing
1999	Lothar	26.1	24.5	9.3	72.0	62.7	80.0%
2002	Jeanette	26.0	27.0	0.0	52.0	52.0	79.3%
2007	Kyrill	26.2	27.0	0.0	56.0	56.0	69.3%
2008	Paula	21.0	21.0	7.7	48.0	40.3	90.6%
2008	Emma	27.1	26.8	10.3	62.0	51.7	67.1%
	Average	25.3	25.3	5.5	58.0	52.5	77.3%

2.1.1 Analysis of peak gust and sustained wind speeds

WMO standards for wind measurement use a disjunctly-sampled sustained wind speed (sampled 10 minutes prior to each hour) and a continuously-sampled gust wind speed. Because of this difference in measurement for the two types of wind speeds, it is possible that the WMO station data does not represent the true sustained wind speeds that were encountered at each location, especially in the event that the highest wind speeds occurred during the first 50 minutes of the hour, illustrated in Figure 2. As demonstrated by this figure,

the average sustained wind speed may be under- or overestimated depending on the fluctuations in the wind storm. For the case of the historic European storms analyzed, it is hypothesized that the WMO station data for sustained wind speeds generally underpredict the actual wind speed. Therefore, both observed peak gust and sustained wind speeds were evaluated to determine if adjustment of the wind data was necessary.

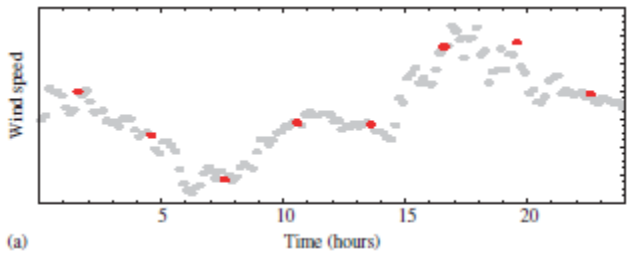

Figure 2. Illustration of the concept of disjunct sampling – in this illustration, the 3 hour wind speed is sampled (dark short lines) from the contiguous 10-min averages (grey short lines) (Larsen and Mann 2006).

To create an equal basis for the sustained and gust wind speeds, the methodology developed by Larsen and Mann (2006) (Equation 1) was used to convert disjunctly-sampled sustained wind speeds to continuous sustained wind speeds with T_d = 1 hour and an averaging time, T_a = 10 minutes.

$$y = \frac{\overline{U^{max}_{N/m\ d,sec}}}{\overline{U^{max}_{N\ sec}}} = b - a(\log_{10}(x))^2 \qquad \text{(Equation 1)}$$

Where x = frequency and $\overline{U^{max}_{N/m\ d,sec}}$ = the average maximum sustained wind speeds from a disjunctively–sampled dataset. The denominator, $U^{max}_{N\ sec}$= represents the average wind maximum. The wind maximum is selected from N data. The coefficients *a* and *b* are calculated using Equations 2 and 3, respectively (Larsen and Mann 2006).

$$a = 0.0209\left(T_d - \frac{1}{6}\right)^{0.4627} \qquad \text{(Equation 2)}$$

$$b = 1 - 0.0342\left(T_d - \frac{1}{6}\right)^{0.5436} \qquad \text{(Equation 3)}$$

To estimate a continuously-sampled 10-minute (3600-second) mean wind speed from the disjunctly-sampled WMO data, Equation 4 was used.

$$U_{3600_{continuous}} = \frac{U_{3600_{disjunct_{measured}}}}{\frac{\overline{U^{max}_{N/m\ d,sec}}}{\overline{U^{max}_{N\ sec}}}} \qquad \text{(Equation 4)}$$

Once the equivalent continuously-sampled sustained wind speed was computed, this value was used to calculate the actual gust factors for the data set for quality control purposes. Implementation of the conversion from a disjunct to continuous sampling basis still revealed inconsistencies in the wind data that could not be explained using the gust factor. A review of the Lothar storm data set found that the actual gust factors (U_3/U_{3600}) calculated from the observed data ranged from 0.89 to 10.17 for the 4258 records (out of 214499 total, 2%) that had both gust and sustained wind speed data available, with an average of 1.83 and a standard deviation of 0.76. Based on the multiple studies discussed earlier in the paper, the expected value is in the range of 1.4. This initial quality control evaluation indicated that the sustained wind speeds were much lower than expected based on the recorded peak gust wind speeds. This necessitated that both the peak gust and sustained wind speed data be used to calculate the final wind speeds used in the interpolation. Therefore, Equations 5 and 6 (or 7) were used to calculate the maximum sustained and peak gust wind speeds using the observed station data.

$$U_{3600} = \max\left(U_{3600_{disjunct_{measured}}}, U_{3_{measured}} \times \frac{U_{3600}}{U_3} \times \frac{\overline{U^{max}_{N/m\ d,sec}}}{\overline{U^{max}_{N\ sec}}}\right) \qquad \text{(Equation 5)}$$

If peak gust measurements are available,

$$U_3 = U_{3_{measured}} \qquad \text{(Equation 6)}$$

If peak gust measurements are not available,

$$U_3 = \frac{U_{3600_{disjunct_{measured}}}}{\frac{\overline{U^{max}_{N/m\ d,sec}}}{\overline{U^{max}_{N\ sec}}}} \times \frac{U_3}{U_{3600}} \qquad \text{(Equation 7)}$$

Where U_3/U_{3600} is the Durst conversion factor (ASCE 7-10 2010). Both the sustained wind speed and peak gust wind speed were evaluated to ensure that errors in data had minimal impact on the final interpolations. Where the maximum sustained wind speed measured was greater than the value calculated using the gust factor and disjunct sample conversion factor,

the measured sustained value was used (Equation 5). For stations that reported peak gust data, these data were used directly (Equation 6), otherwise a peak gust wind speed was calculated using the gust factor and disjunct sample conversion factor (Equation 7). Using these algorithms, the Lothar dataset was again evaluated as a test case. The results show that the methodology does not significantly overpredict the gust wind speed data (an average increase of 2%, standard deviation of 5%). Further, the methodology accounted for the underreporting of sustained wind speeds because of the disjunct sampling period. The final gust factors (U_3/U_{3600}) for the calculated dataset were reevaluated and were found to range from 1 to 1.4299, with an average of 1.42 and a standard deviation of 0.03 for the 4258 records. Although low gust factors (<1.4) were seen for approximately 5% of the data, this methodology created a dataset that was more consistent. These results demonstrate that the implemented calculation methodology produces wind speeds that are more consistent with standard wind engineering metrics.

2.1.2 Covariate data

Additionally, covariate data from Europe were obtained for the cokriging process. Elevation data were collected from Version 4 of the NASA Shuttle Radar Topographic Mission (SRTM) 90-m digital elevation dataset through the CGIAR Consortium for Spatial Information (CGIAR-CSI). The land cover covariate was obtained from the European Space Agency (ESA) GlobCover Project Version 2 2008 database at a resolution of 300 meters (GlobCover 2008). Collectively, the elevation and land cover datasets were clipped and resampled to 300 meters for the study area. The GlobCover land cover dataset contains 22 different land cover classification types ranging from various tree types, shrubs, and grasslands to bare land, artificial surfaces, and open water. The covariate of aspect was derived from the 300-m resampled elevation dataset utilizing tools available in the Spatial Analyst toolbox within ArcMap 10.1.

2.2 Kriging and cokriging methodologies

Kriging and cokriging rely on probability and autocorrelation when creating surface estimates. The use of probability means that there is some variation in output values leading to an approximate, or stochastic, model. The reliance on autocorrelation is based on the tendency for two variables to be related. Within the field of geography, Tobler's first law states that "everything is related to everything else, but near things are more related than

distant things" (Tobler 1970). Correlation between objects usually decreases over distance and this is also true of the correlation between wind speeds at different stations. Autocorrelation is a central tenet of geostatistics because observations are not independent of each other and geostatistics includes spatial location and distance during model creation. Kriging and cokriging both rely on the same process for surface estimation, but cokriging incorporates one or more secondary variables to improve predictions in areas where simple autocorrelation may be insufficient. Larger wind speed values may be underestimated in mountainous or coastal areas that lack a dense network of wind observation stations. However, even when considering station location limitations, cokriging has been shown to estimate wind surfaces more accurately and in greater detail, while reducing prediction errors, compared to ordinary kriging (Luo et al. 2008).

While ordinary kriging is described as

$$Z(\mathbf{s}) = \mu + \varepsilon(\mathbf{s})$$

where constant mean μ is a deterministic trend that is associated with errors ε at each location **s** for the variable of interest $Z(\mathbf{s})$, ordinary cokriging is described as

$$Z_1(\mathbf{s}) = \mu_1 + \varepsilon_1(\mathbf{s})$$
$$Z_2(\mathbf{s}) = \mu_2 + \varepsilon_2(\mathbf{s})$$
$$Z_n(\mathbf{s}) = \mu_n + \varepsilon_n(\mathbf{s})$$

where constants $\mu_1 \ldots \mu_n$ are unknown and associated with multiple errors ε_n at each location **s** to predict variable of interest $Z_1(\mathbf{s})$, while taking information from covariate(s) $Z_n(s)$ into consideration.

In cokriging, different trends are estimated for each variable and autocorrelation occurs within each variable, while cross-correlation can also occur between the errors for each variable. Measurement locations do not need to be the same when the level of cross-correlation is calculated between variables – a major advantage of cokriging. Cokriging utilizes autocorrelation and cross-correlation to often make improved predictions, but the addition of one or more secondary variables (covariates) requires more estimation of unknown autocorrelation parameters and adds more model variability. However, the cokriging model is based on the kriging model and if no cross-correlation exists, the original autocorrelation remains the baseline. This infers that cokriging models will not underperform compared to kriging models, but occasionally the added model variability of cokriging can increase standard error on a station-by-station basis. Within kriging, random errors assume second-order stationarity indicating that errors have a mean of zero and error covariance is not location-dependent, but instead is distance- and direction-dependent. In addition to ordinary cokriging, other methods of cokriging exist that include universal, simple, indicator, probability, and disjunctive. These methods offer slight changes to the ordinary cokriging methodology such as the ability to use multiple data thresholds, prediction thresholds, and variable trends.

Although normally distributed data are not required for kriging, normality is necessary to obtain quantile and probability maps. Additionally, kriging is the optimal unbiased predictor when compared to only techniques produced from weighted averages regardless of data normality, but if the data are normally distributed then kriging is the optimal predictor compared to all other unbiased predictors. The data were examined to determine if a transformation or other corrections were necessary to produce normally distributed data and to ensure that kriging is the "best" prediction compared to other unbiased predictors. Prior to modeling each wind storm, multiple methods of exploratory spatial data analysis (ESDA) were employed using the Geostatistical Analyst within ArcMap 10.1 to examine the univariate distribution (histogram), stationarity and spatial variability (Voronoi map), normality (normal QQ plot), global trends (trend analysis), and spatial dependencies (semivariogram/covariance cloud) of the wind observation data as well as the autocorrelation between covariates and between wind observation data and covariates (general QQ plot and crosscovariance cloud). The levels of skewness and kurtosis revealed by ESDA indicated that the wind observation data deviates slightly from a normal distribution. Observational data were subsequently tested for normality using the Shapiro-Wilk test (Sliz-Szkliniarz and Vogt 2011). The Shapiro-Wilk test examines the null hypothesis that a dataset is distributed normally. Values below a certain alpha level (e.g., $p < 0.05$) indicate that the null hypothesis of normality should be rejected and values above a certain alpha level indicate the opposite.

Anisotropic semivariograms were created during the interpolation procedure to account for directional dependence of wind speeds at varying distances. Dominant directional trends were automatically detected for each storm and wind type. This most often resulted in directional trends that logically corresponded to storm tracks, but occasionally dominant trends were difficult to determine and directionality was adjusted accordingly. Additionally, a variable search radius was determined based on an optimized number of points through cross-validation using the Geostatistical Analysis tool in ArcGIS Version 9.3 (ESRI 2010). A radius of 15 points was determined to adequately reflect spatial covariance, meaning that appropriate range and sill values could be determined by incorporating this number of points to estimate local surface trends similar to a moving window. For semivariogram surface creation, an eight sector elliptical search type with three neighbors per sector was specified to optimize surface variability.

The interpolation parameters were selected to obtain the highest accuracy based on the station data. Multiple measures of accuracy including ME, RMSE, and minimum/maximum range were used to determine the validity of each kriging-derived surface, but these statistical

measures only measure the accuracy as it is related to observed and estimated variability of wind speed on the surface. The standardized RMSE and ME as well as the minimum/maximum surface estimates were used to evaluate the interpolated surface and compare the accuracy for each storm. Relatively lower values (close to 0) for ME and values closest to 1 for RMSE are preferred. A wider minimum/maximum range estimate infers more variability in wind speeds across the interpolated surface, while a narrower minimum/maximum range estimate infers more conformity in wind speeds across the interpolated surface. Negative ME values infer that variability was underestimated, while positive ME values infer variability was overestimated. RMSE values less than 1 infer that variability was overestimated, while RMSE values greater than 1 infer that variability was underestimated. The standard error of each station (standard deviation from mean) was also used as a major indicator of inter-model comparison. Standard errors that were > +/-2.0 were considered to be abnormally high and a major goal of cokriging was to reduce the number of stations that reported a high standard error. The number of stations with "abnormally high" standard error were summated for each model and used as an indicator of model improvement. Additionally, automatic anisotropy was calculated for each storm to compare to actual storm direction. Automatic azimuth directions that were closer to actual storm paths were considered optimal. In addition to measuring the accuracy of the interpolated surfaces variability, storm tracks and other reports were used to validate the actual trends, locations, and magnitudes of estimated wind speeds.

3. Results

3.1 Cokriging assessment and evaluation

Maximum sustained and peak gust wind speeds were analyzed for each of the five studied wind storms to determine whether pre-processing data transformations were necessary and to determine the best combinations of covariates that produce optimal wind surface estimates based on multiple criteria. The Shapiro-Wilk test for normality revealed that the null hypothesis of normality for each station could not be rejected since *p*-values were greater than 0.05 for each storm and wind type (Table 6). Based on the results of the Shapiro-Wilk test, no data transformations were necessary for the station observation data. Additionally, regression analysis revealed extremely low *R*-values ($R < 0.1$) and no values were significant ($p > 0.05$) between covariates and between wind observation data and covariates indicating

that autocorrelation is not a major issue and that transformation of the covariates was unnecessary. The ESDA tools within Geostatistical Analyst also revealed trends for each wind storm dataset. These trends were generally consistent with expected directional trends based on the track of each wind storm resulting in west-east or northwest-southeast tendencies.

Table 6. Shapiro-Wilk test for normality for each storm and wind type

Storm	Wind Type	Shapiro-Wilk (W)	*p*-value	Reject H_0
Lothar	Max Sustained	0.997	0.79	No
	Peak Gust	0.995	0.38	No
Jeanette	Max Sustained	0.997	0.08	No
	Peak Gust	0.999	0.89	No
Kyrill	Max Sustained	0.999	0.97	No
	Peak Gust	0.998	0.84	No
Paula	Max Sustained	0.998	0.47	No
	Peak Gust	0.998	0.70	No
Emma	Max Sustained	0.998	0.94	No
	Peak Gust	0.996	0.22	No

Daily weather maps and other climatological information from various reports were utilized to assess the track and synoptic conditions and gather a more holistic view for each wind storm. Ordinary cokriging was employed for each storm and wind type and every possible covariate combination was simulated. The maximum amount of combinations resulted in eight interpolated surfaces for each wind type and 16 total interpolated surfaces for each storm. These eight interpolated surfaces included 1) ordinary kriging without covariates, 2) cokriging with elevation, 3) cokriging with aspect, 4) cokriging with land cover, 5) cokriging with elevation and aspect, 6) cokriging with elevation and land cover, 7) cokriging with aspect and land cover, and 8) cokriging with elevation, aspect, and land cover. Corresponding maps were created to represent the maximum sustained and peak gust wind speeds across the region for the duration of each storm. Accuracy metrics were calculated through a process of cross validation (n - 1) during model simulation and included the RMSPE, ME, RMSE, and stations with errors greater than +/- 2.0 standard deviations. Automatic wind direction trends were also recorded. Additional maps were also created for each storm and wind type to identify the locations of stations that received high errors from each cokriging model. The optimal model output(s) was (were) determined for each storm and wind type.

3.2 Cokriging models

3.2.1 Wind storm Lothar

Wind storm Lothar was the first of two major storms to impact northwestern Europe in 1999. A subsequent storm, Martin, followed nearly the same path just one day later. Lothar developed from a depression in the North Atlantic Ocean and collided with a cold air mass on land, resulting in increased surface turbulence along the frontal boundary and the rapid development and geographic expansion of Lothar. The wind storm moved from west to east with major damage occurring in France, Germany, Switzerland, and Austria. Approximately 140 deaths and €10 billion (euros) in damage were attributable to Lothar and Martin collectively (EQE 2000). It is difficult to parse which storm caused the most direct damage, but Lothar was the stronger of the two. During Lothar, several wind observation stations reported gust wind speeds in excess of 40 m s^{-1} – comparable to Category 2 hurricane wind speeds. Building roofs, communication networks, and fruit trees were particularly hard-hit by high wind speeds, while avalanches, mudslides, and flooding also occurred (EQE 2000). A deadly avalanche in Galtuer, Austria, resulted in nine deaths.

The results of cokriging models for maximum sustained (Figure 3) and peak gust (Figure 4) wind speeds provided additional evidence of the general west-east storm track for Lothar. Wind speeds approaching 40 m s^{-1} were estimated by multiple peak gust models in coastal areas of France and mountainous areas of southeastern Germany approaching the Austrian Alps. Some differences in wind speed estimates were observed between most surfaces. For example, Figures 3a and 3c showed higher maximum sustained wind speed estimates in southeastern Germany, while most models estimated a decline in wind speeds across northeastern France before a reversion to increased wind speeds near Switzerland and southwestern Germany. Figure 4c showed higher peak gust wind speed estimates in southeastern Germany, while Figure 4b showed a very spotty surface with smaller, more emphasized areas of high and low wind speeds.

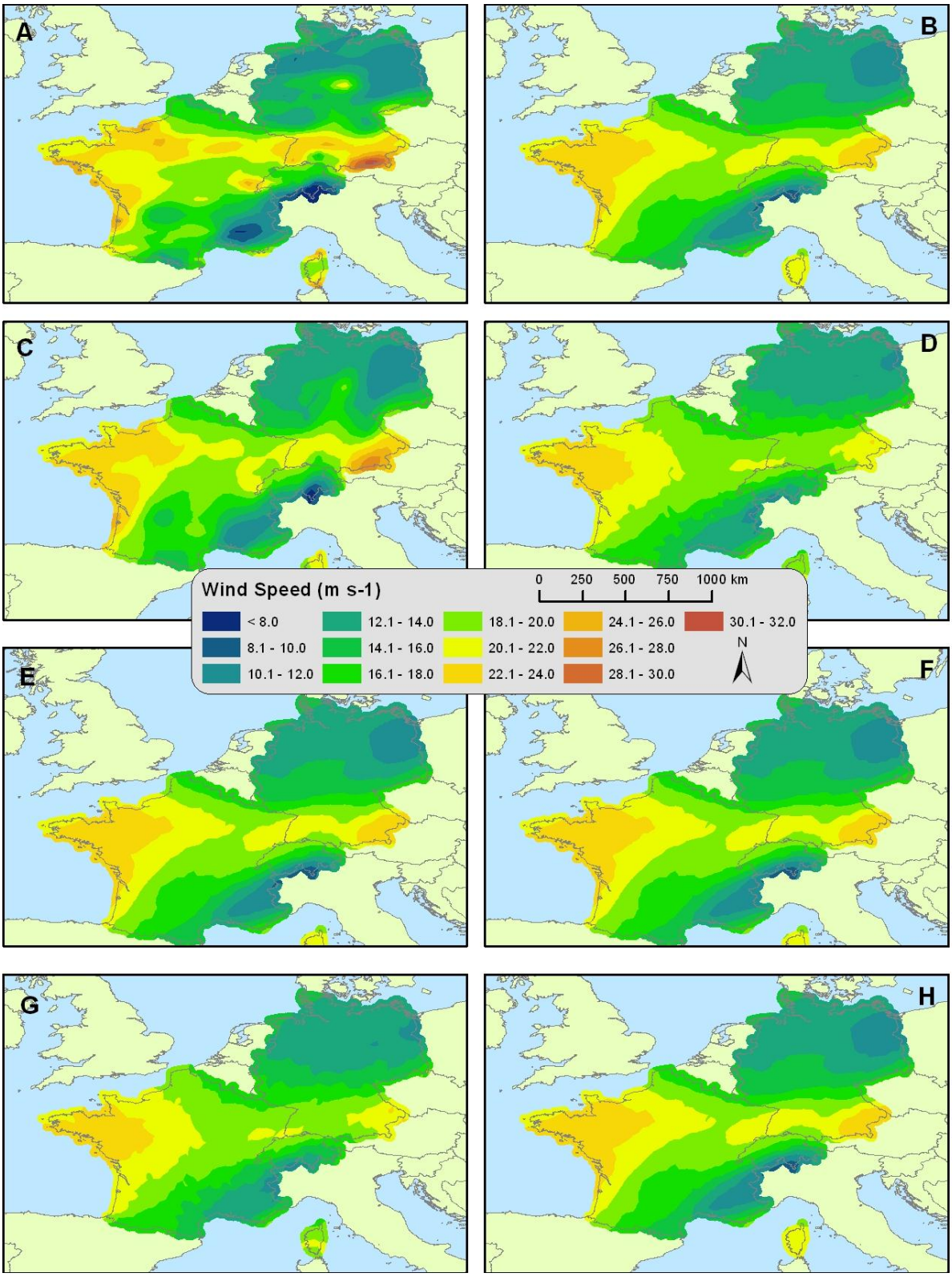

Figure 3. Maximum sustained wind surface estimates for wind storm Lothar produced by the following models: original kriging (A), cokriging with elevation (B), cokriging with aspect (C), cokriging with land cover (D), cokriging with elevation and aspect (E), cokriging with elevation and land cover (F), cokriging with aspect and land cover (G), and cokriging with elevation, aspect, and land cover (H).

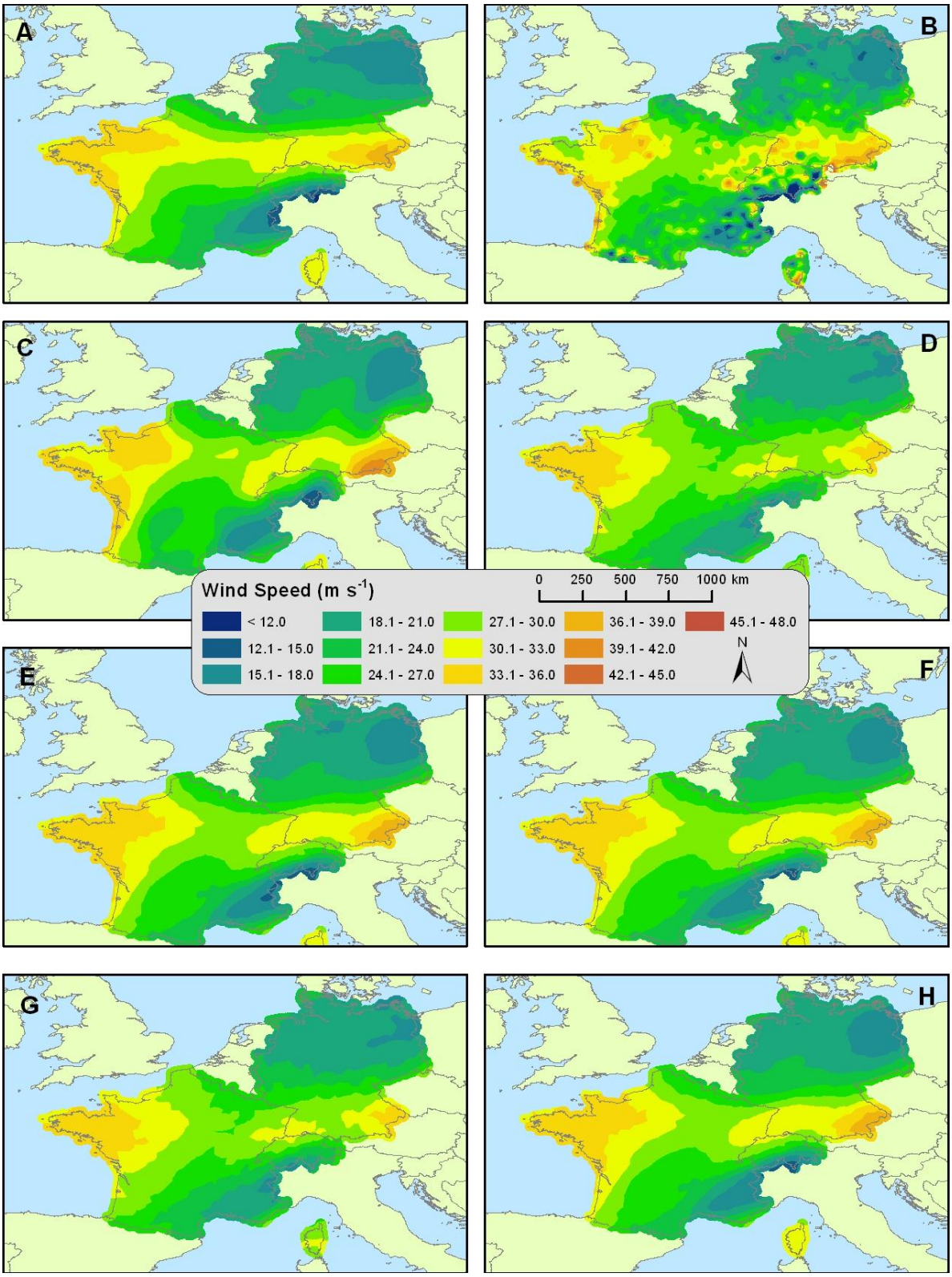

Figure 4. Peak gust wind surface estimates for wind storm Lothar produced by the following models: original kriging (A), cokriging with elevation (B), cokriging with aspect (C), cokriging with land cover (D), cokriging with elevation and aspect (E), cokriging with elevation and land cover (F), cokriging with aspect and land cover (G), and cokriging with elevation, aspect, and land cover (H).

To determine the optimal model(s) for each wind speed type for wind storm Lothar, multiple accuracy metrics were utilized during model implementation. The accuracy metrics for each model and wind type were aggregated in Table 7. For the wind storm Lothar maximum sustained wind models, the original kriging methodology produced the automated anisotropic conditions closest to the actual storm track of ~90°. The model utilizing the covariate aspect produced the RMSE score nearest to one and the lowest RMSPE score, while the ME nearest to zero was produced by the model utilizing aspect and land cover. All models except two (original kriging and cokriging with aspect) reported the fewest high station SE measurements (14) after cross-validation. For the peak gust wind models, the original kriging methodology again produced the automated anisotropic conditions closest to the actual storm track of ~90°. The original kriging model also produced the RMSE score nearest one and tied five other models with the fewest stations reporting a SE measurement of greater than +/-2.0. The model utilizing elevation as a covariate received the lowest RMSPE score, while the ME nearest to zero was produced by the model incorporating land cover.

Table 7. Wind storm Lothar accuracy metrics.

Storm	Method	Anisotropy	RMSPE	ME	RMSE	SE (> +/- 2.0)
Lothar	Original Kriging	81.4	6.34	-0.010	1.03	18
Max	Cokriging w/elev	70.5	6.35	0.004	0.97	14
Sustained	Cokriging w/asp	45.4	6.32	0.004	1.00	16
	Cokriging w/LC	63.5	6.55	0.003	0.95	14
	Cokriging w/elev & asp	70.5	6.35	0.004	0.97	14
	Cokriging w/elev & LC	70.3	6.35	0.005	0.97	14
	Cokriging w/asp & LC	63.8	6.55	0.002	0.95	14
	Cokriging w/elev, asp, & LC	70.3	6.35	0.005	0.97	14
Lothar	Original Kriging	84.9	10.31	0.002	1.00	16
Peak	Cokriging w/elev	78.4	9.81	-0.030	1.04	20
Gust	Cokriging w/asp	55.2	10.31	0.002	1.02	20
	Cokriging w/LC	63.5	10.58	0.001	0.97	16
	Cokriging w/elev & asp	70.5	10.29	0.002	0.99	16
	Cokriging w/elev & LC	70.3	10.29	0.003	0.99	16
	Cokriging w/asp & LC	63.5	10.59	0.002	0.97	16
	Cokriging w/elev, asp, & LC	70.3	10.29	0.003	0.99	16

To examine in more detail the locations of stations where high SE measurements occurred, maps were produced for each wind type for wind storm Lothar (Figure 5a-b). Most stations that received high SE measurements received such measurements from multiple models. For the maximum sustained wind speed models, high SE measurements were

recorded by stations in mountainous regions of Switzerland and southern Germany approaching Austria as well as one station in the French Pyrenees. Some stations on the island of Corse also reported high SE measurements. For the peak gust wind speed models, high SE measurements were recorded in near- identical areas in mountainous regions, while the Atlantic and Mediterranean coasts of France also contained stations with high SE measurements. Stations coinciding with the optimal models based on SE measurements were also highlighted and occurred in matching mountainous and coastal areas.

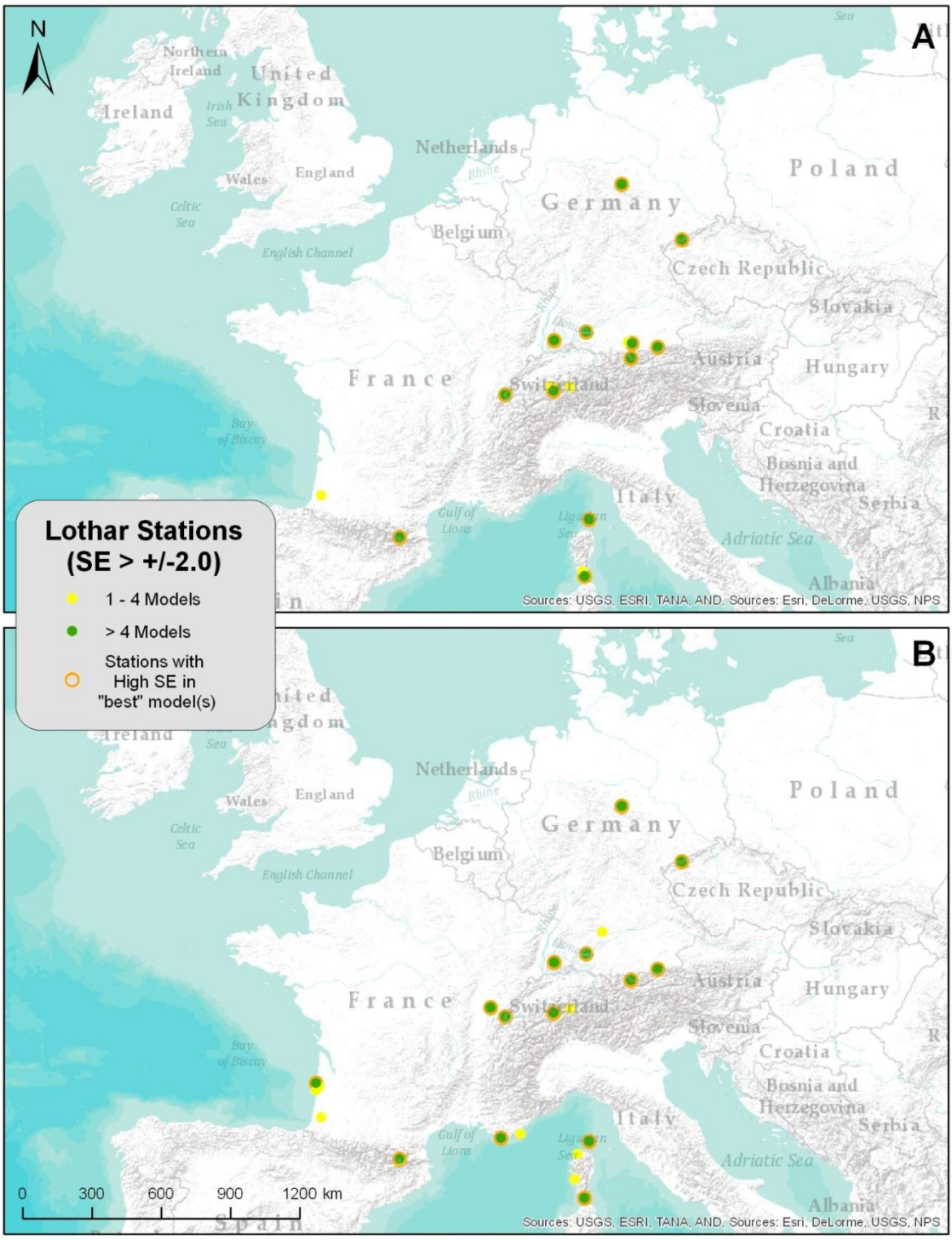

Figure 5. Locality of stations reporting high SE measurements for maximum sustained (A) and peak gust (B) winds.

3.2.2 Wind storm Jeanette

Wind storm Jeanette impacted much of northern Europe in late October of 2002 as it tracked across Ireland, the UK, North Sea, Denmark, and Sweden. Jeanette developed from a low pressure system in the North Atlantic Ocean and had a long, attached frontal boundary that reached deep into southern Europe. Because of the size of the storm and extent of the frontal boundary, Jeanette impacted more countries in Europe than most other wind storms with high winds distributed over relatively large areas. The wind storm moved from west to east with major damage occurring in Ireland, the UK, France, Belgium, the Netherlands, Germany, Denmark, Sweden, Switzerland, Austria, Czech Republic, and Poland. Approximately 30 deaths and €1.5 billion (euros) in damage were attributable to Jeanette with insured losses topping €1 billion (EQECAT 2002, RMS 2002). The biggest losses occurred in the western and eastern coastal UK, Belgium, the Netherlands, and northern and eastern Germany. During Jeanette, several wind observation stations in France, the Netherlands, Germany, and Poland reported gust wind speeds in excess of 40 m s^{-1} – comparable to Category 2 hurricane wind speeds. Buildings, communication and transport networks, power lines and trees were particularly hard-hit by high wind speeds, while flooding was a major concern in Scotland and England (EQECAT 2002).

The results of cokriging models for maximum sustained (Figure 6) and peak gust (Figure 7) wind speeds provided additional evidence of the general west-east storm track for Jeanette. Wind speeds approaching 33 m s^{-1} were estimated by multiple peak gust models in coastal areas of the UK, Belgium, and the Netherlands. High wind speeds persisted across much of central Germany, with wind speeds actually increasing in eastern Germany near the Czech Republic border (Figure 7c). Some differences in wind speed estimates were observed between most surfaces. For example, Figures 6c and 6d showed variation in how far inland the highest wind speeds occurred in eastern Germany, while most models estimated that higher wind speeds were maintained through Germany to the Czech Republic. Figure 7c showed higher peak gust wind speed estimates in eastern Germany, while other peak gust models did not identify this area of higher winds.

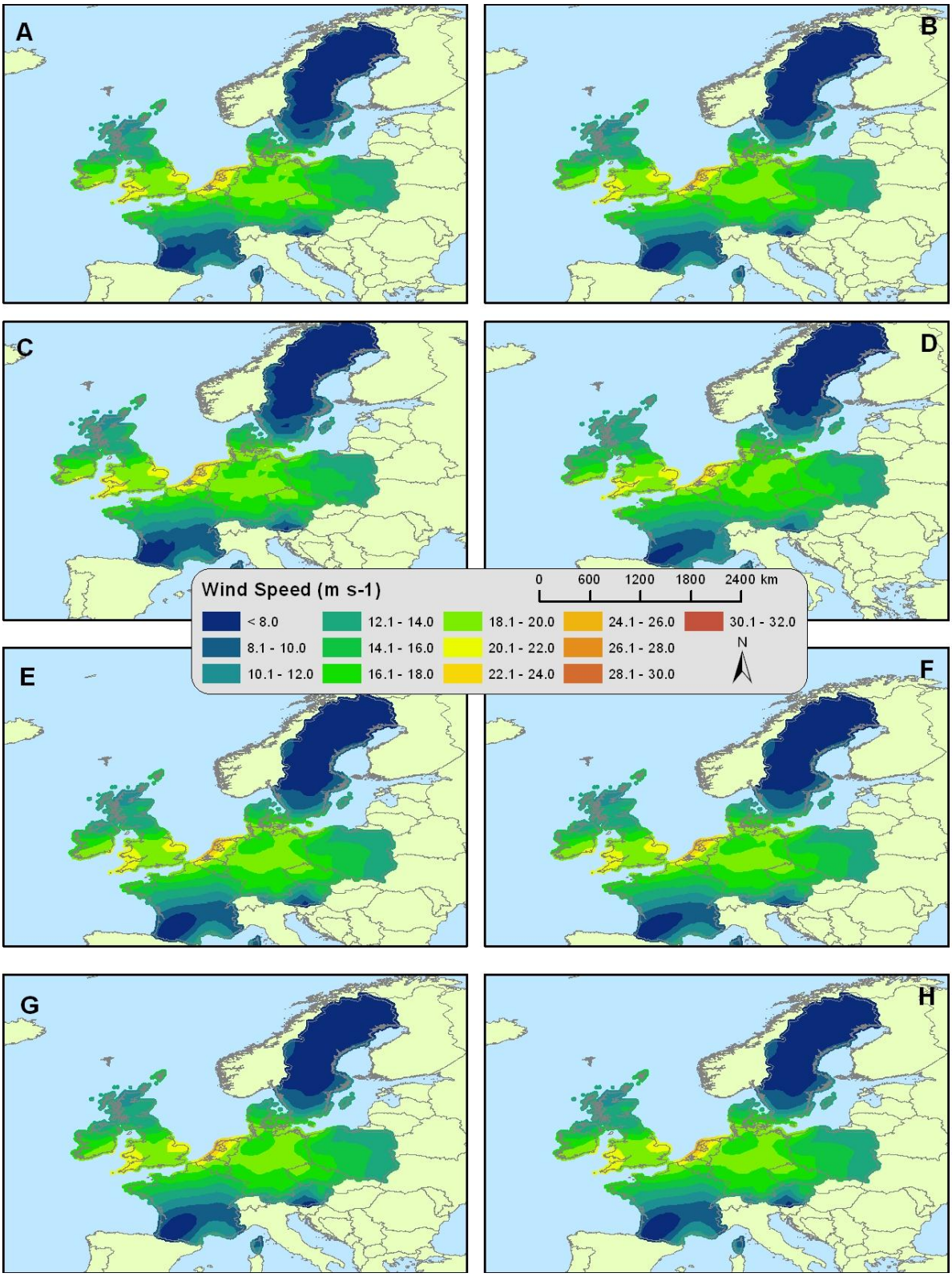

Figure 6. Maximum sustained wind surface estimates for wind storm Jeanette produced by the following models: original kriging (A), cokriging with elevation (B), cokriging with aspect (C), cokriging with land cover (D), cokriging with elevation and aspect (E), cokriging with elevation and land cover (F), cokriging with aspect and land cover (G), and cokriging with elevation, aspect, and land cover (H).

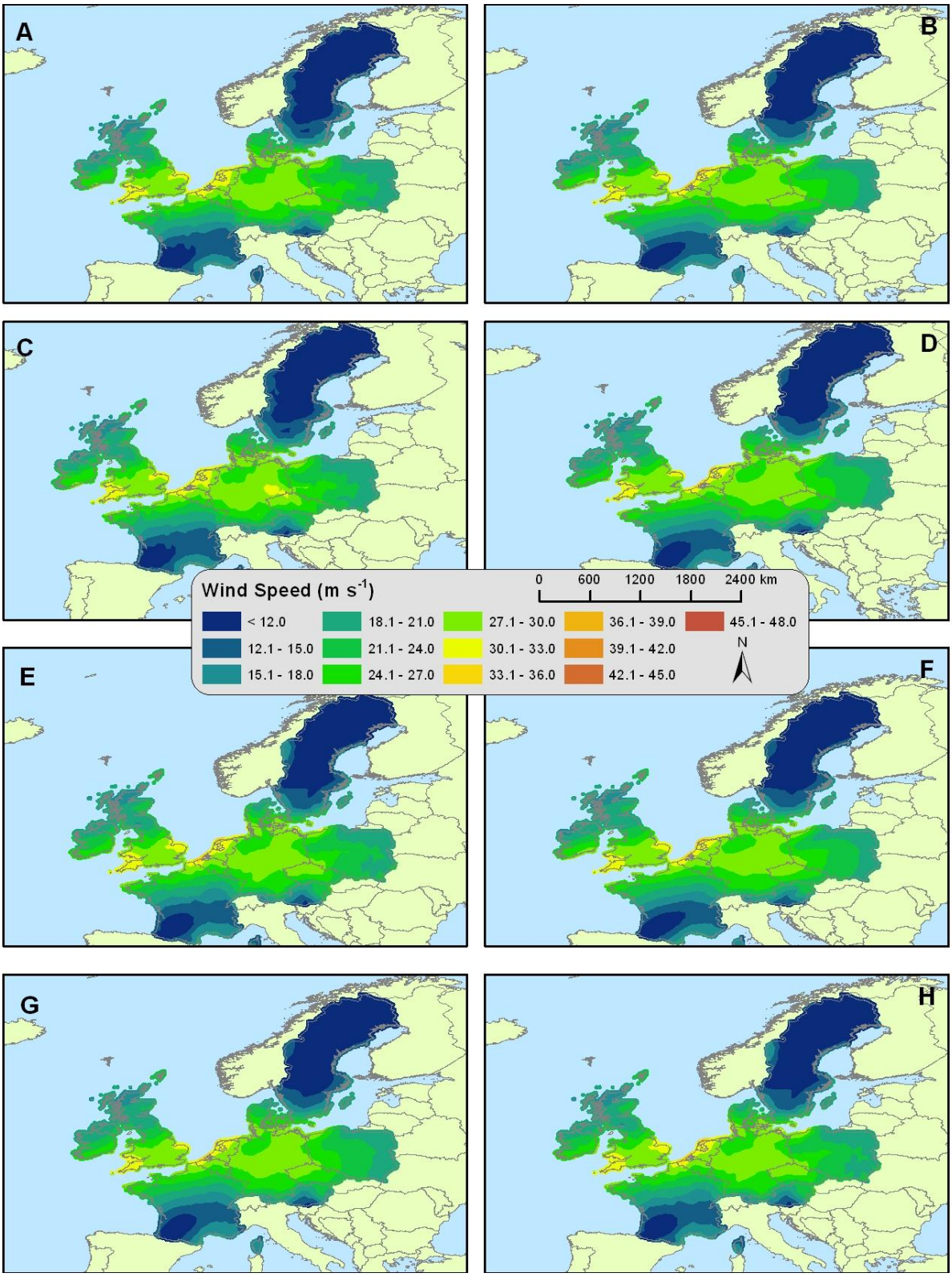

Figure 7. Peak gust wind surface estimates for wind storm Jeanette produced by the following models: original kriging (A), cokriging with elevation (B), cokriging with aspect (C), cokriging with land cover (D), cokriging with elevation and aspect (E), cokriging with elevation and land cover (F), cokriging with aspect and land cover (G), and cokriging with elevation, aspect, and land cover (H).

To determine the optimal model(s) for each wind speed type for wind storm Jeanette, multiple accuracy metrics were utilized during model implementation. The accuracy metrics for each model and wind type were aggregated in Table 8. For the wind storm Jeanette maximum sustained wind models, three models (original kriging, cokriging with aspect, and cokriging with elevation and aspect) produced the automated anisotropic conditions closest to the actual storm track of ~85°. Three models (cokriging with elevation, cokriging with elevation and aspect, cokriging with all three covariates) also produced the lowest RMSPE score, while the ME nearest to zero was produced by five of the eight models. The model that utilized cokriging with elevation and land cover produced the RMSE score nearest one, while the cokriging model incorporating only land cover reported the fewest stations with high SE measurements (26) after cross-validation. For the peak gust wind models, the original kriging model and the cokriging model utilizing aspect produced the automated anisotropic conditions closest to the actual storm track of ~85°. Multiple models produced the lowest RMSPE score of 7.80, while three models (cokriging with land cover, cokriging with elevation and land cover, and cokriging with aspect and land cover) received the ME score nearest zero. The cokriging model that included elevation and the cokriging model that included elevation and land cover received the RMSE score nearest one. The cokriging model that utilized elevation and aspect together resulted in the fewest stations (19) reporting a SE measurement of greater than +/-2.0.

Table 8. Wind storm Jeanette accuracy metrics.

Storm	Method	Anisotropy	RMSPE	ME	RMSE	SE (> +/- 2.0)
Jeanette	Original Kriging	90.0	4.78	0.001	0.87	29
Max	Cokriging w/elev	71.8	4.77	0.001	0.96	37
Sustained	Cokriging w/asp	90.0	4.78	0.008	0.87	29
	Cokriging w/LC	64.3	4.84	-0.001	0.89	26
	Cokriging w/elev & asp	80.0	4.77	0.001	0.96	37
	Cokriging w/elev & LC	69.6	4.78	0.002	0.97	36
	Cokriging w/asp & LC	74.5	4.78	0.001	0.94	35
	Cokriging w/elev, asp, & LC	74.1	4.77	0.011	0.96	37
Jeanette	Original Kriging	90.0	7.80	0.007	0.87	33
Peak	Cokriging w/elev	69.6	7.82	0.002	0.96	38
Gust	Cokriging w/asp	90.0	7.80	0.006	0.86	32
	Cokriging w/LC	62.6	7.80	0.001	0.93	38
	Cokriging w/elev & asp	76.9	7.83	0.008	0.72	19
	Cokriging w/elev & LC	69.6	7.82	0.001	0.96	38
	Cokriging w/asp & LC	63.2	7.80	0.001	0.93	38
	Cokriging w/elev, asp, & LC	78.1	7.84	0.009	0.72	20

To examine in more detail the locations of stations where high SE measurements occurred, maps were produced for each wind type for wind storm Jeanette (Figure 8a-b). Most stations that received high SE measurements received such measurements from multiple models. For the maximum sustained wind speed models, high SE measurements were recorded by stations in mountainous regions of Austria and southern Germany as well as the northern Czech Republic and Scotland. Coastal areas of the UK, France, Germany, and Poland also reported stations with high SE measurements from multiple stations. For the peak gust wind speed models, high SE measurements were recorded in near-identical areas in mountainous and coastal regions with the addition of several stations along the coast of the Netherlands. Stations coinciding with the optimal model(s) based on SE measurements were also highlighted and continued to exhibit a mountainous and coastal presence.

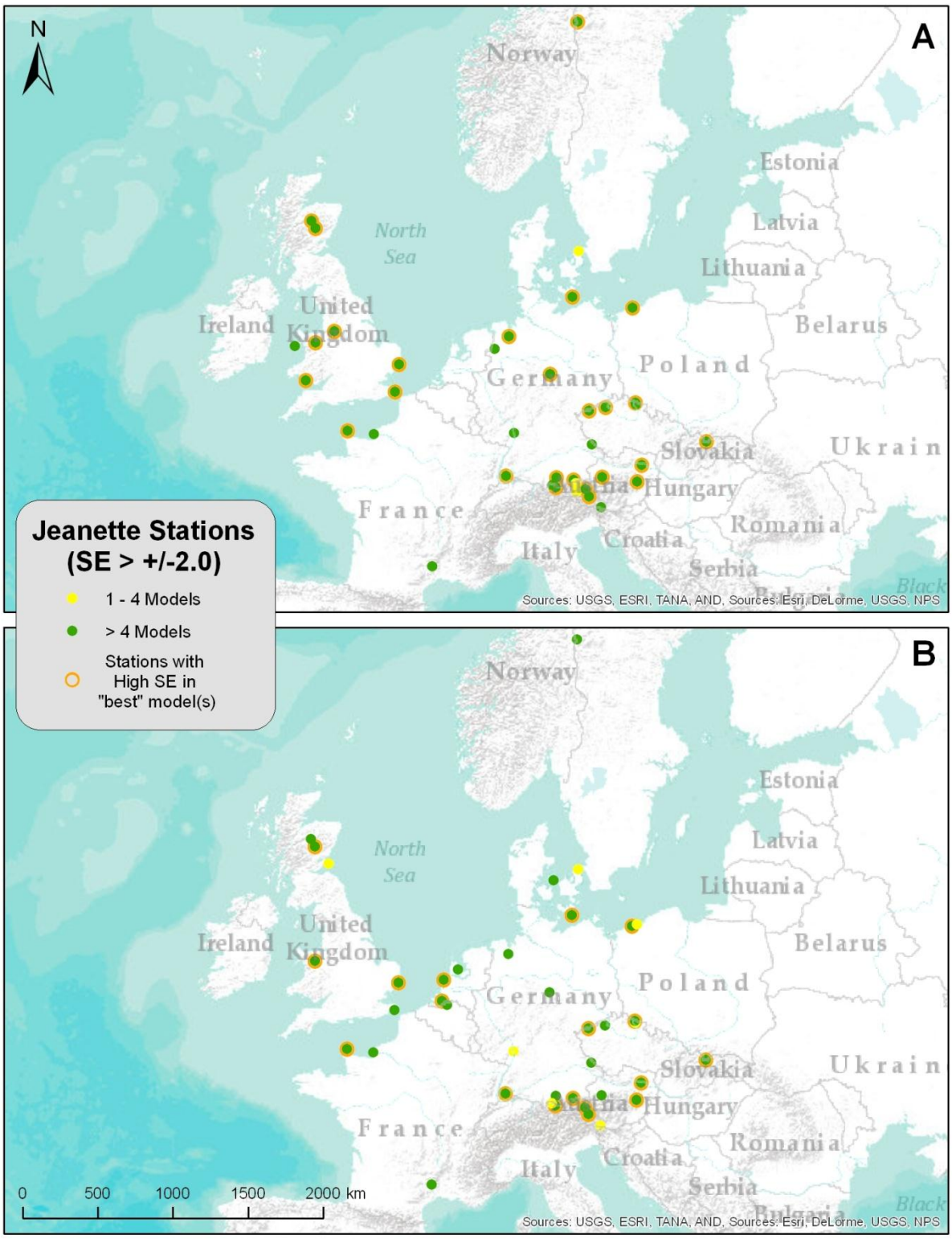

Figure 8. Locality of stations reporting high SE measurements for maximum sustained (A) and peak gust (B) winds.

3.2.3 Wind storm Kyrill

Wind storm Kyrill impacted large areas of northern Europe in January 2007 as it took a track similar to that of wind storm Jeanette across Ireland, the UK, North Sea, Denmark, and Germany. Kyrill developed from a low pressure system near Newfoundland in northeastern Canada on 15 January and moved across the North Atlantic Ocean before making its first landfall in Ireland on 17 January. Hurricane-force winds extended very far from the center of the storm and widespread major damage occurred as a result of these extensive high winds. The wind storm moved from west to east with substantial damage reported in the UK, France, Belgium, the Netherlands, Germany, Austria, Czech Republic, and Poland. Approximately 47 deaths and €5 billion (euros) in damage were attributable to Kyrill with insured losses nearing €3.5 billion (EQECAT 2007, Hewston 2007). The biggest losses occurred in the southern UK and throughout most of Germany. During Kyrill, isolated wind observation stations in Germany, Poland, and the Czech Republic reported gust wind speeds in excess of 50 m s^{-1} – comparable to Category 3 hurricane wind speeds. Buildings, communication and transport networks, power lines, and trees suffered major damage from high wind speeds, while flooding was a major concern in Ireland and the Netherlands (EQECAT 2007, Hewston 2007). Additionally, high winds over the Alps produced föhn (foehn) winds (high, downslope winds that cause rapid adiabatic warming of air) across Austria and Italy resulting in avalanche warnings and road tunnel closures.

The results of cokriging models for maximum sustained (Figure 9) and peak gust (Figure 10) wind speeds provided additional evidence of the general west-east storm track for Kyrill. Wind speeds approaching 36 m s^{-1} were estimated by several peak gust models in coastal areas of the UK, the Netherlands, and central/eastern Germany. High wind speeds persisted across much of central Germany, with all models indicating an increase in wind speed as the storm tracked eastward towards the Czech Republic. Some differences in wind speed estimates were observed between most surfaces. For example, Figures 9d and 9g do not show wind speeds over 20 m s^{-1} in eastern Germany, while all other maximum sustained and peak gust models estimated that wind speeds increased across central and eastern Germany. Figures 9c and 10a show the highest maximum sustained and peak gust wind speed estimates in central and eastern Germany.

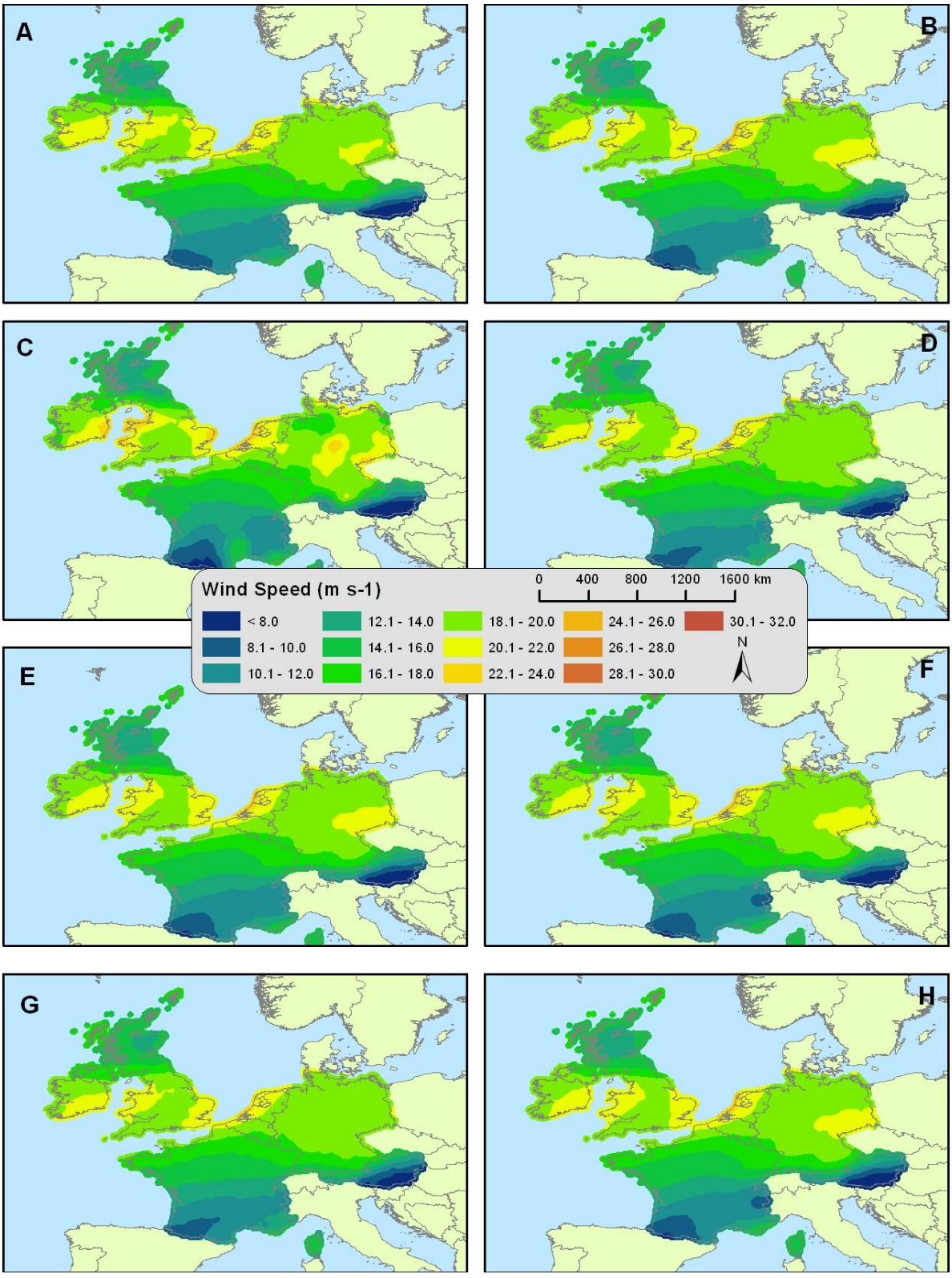

Figure 9. Maximum sustained wind surface estimates for wind storm Kyrill produced by the following models: original kriging (A), cokriging with elevation (B), cokriging with aspect (C), cokriging with land cover (D), cokriging with elevation and aspect (E), cokriging with elevation and land cover (F), cokriging with aspect and land cover (G), and cokriging with elevation, aspect, and land cover (H).

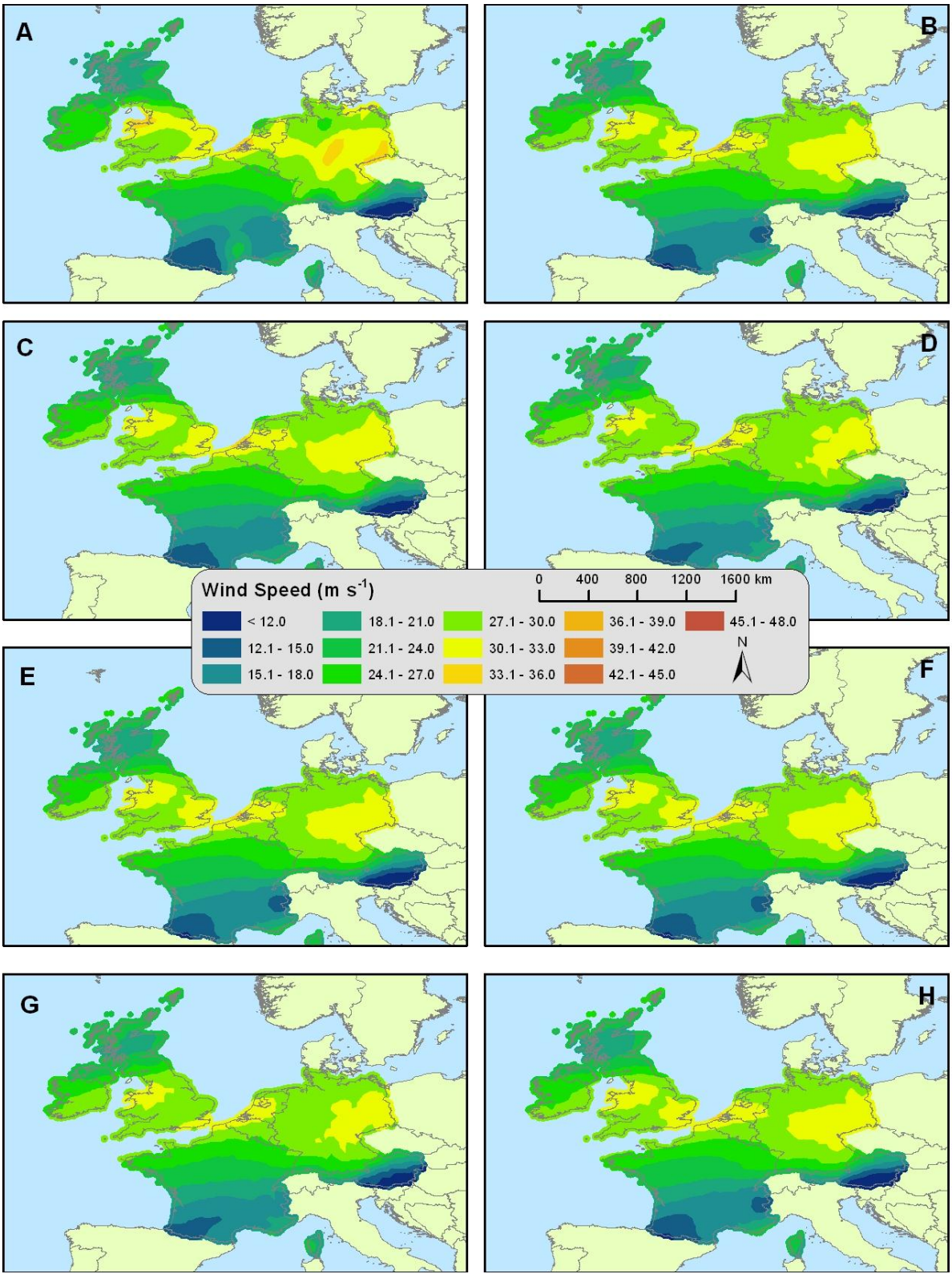

Figure 10. Peak gust wind surface estimates for wind storm Kyrill produced by the following models: original kriging (A), cokriging with elevation (B), cokriging with aspect (C), cokriging with land cover (D), cokriging with elevation and aspect (E), cokriging with elevation and land cover (F), cokriging with aspect and land cover (G), and cokriging with elevation, aspect, and land cover (H).

To determine the optimal model(s) for each wind speed type for wind storm Kyrill, multiple accuracy metrics were utilized during model implementation. The accuracy metrics for each model and wind type were aggregated in Table 9. For the wind storm Kyrill maximum sustained wind models, the original kriging methodology produced the automated anisotropic conditions closest to the actual storm track of ~82°. The cokriging models utilizing elevation, elevation and aspect, elevation and land cover, and all three covariates the lowest RMSPE score and the RMSE score nearest to one. Three cokriging models (aspect, elevation and aspect, and all three covariates) produced the ME nearest to zero. The cokriging model utilizing only aspect reported the fewest stations (35) with high SE measurements. For the peak gust wind models, the cokriging model utilizing aspect produced the automated anisotropic conditions closest to the actual storm track of ~82°, while the cokriging model utilizing aspect and land cover received the ME score nearest to zero. The original kriging model produced the lowest RMSPE score and the fewest stations (37) reporting a SE measurement of greater than +/-2.0. Half of the models received the RMSE score nearest to one.

Table 9. Wind storm Kyrill accuracy metrics.

Storm	Method	Anisotropy	RMSPE	ME	RMSE	SE (> +/- 2.0)
Kyrill	Original Kriging	80.3	4.44	0.016	0.98	39
Max	Cokriging w/elev	68.2	4.39	0.009	0.99	41
Sustained	Cokriging w/asp	72.1	4.40	0.008	0.93	35
	Cokriging w/LC	64.0	4.46	0.015	0.97	41
	Cokriging w/elev & asp	68.2	4.39	0.009	0.99	41
	Cokriging w/elev & LC	68.0	4.39	0.008	0.99	41
	Cokriging w/asp & LC	64.2	4.46	0.013	0.97	40
	Cokriging w/elev, asp, & LC	68.0	4.39	0.008	0.99	41
Kyrill	Original Kriging	64.8	7.16	0.003	0.94	37
Peak	Cokriging w/elev	68.2	7.19	0.005	0.99	43
Gust	Cokriging w/asp	71.6	7.19	0.005	0.96	38
	Cokriging w/LC	64.2	7.24	0.001	0.96	40
	Cokriging w/elev & asp	68.2	7.19	0.005	0.99	43
	Cokriging w/elev & LC	68.2	7.20	0.005	0.99	42
	Cokriging w/asp & LC	64.5	7.23	0.000	0.96	40
	Cokriging w/elev, asp, & LC	68.2	7.19	0.005	0.99	43

To examine in more detail the locations of stations where high SE measurements occurred, maps were produced for each wind type for wind storm Kyrill (Figure 11a-b). Most stations that received high SE measurements received such measurements from multiple

models. For the maximum sustained wind speed models, high SE measurements were recorded by stations in mountainous regions of Austria and southern Germany as well as coastal and interior areas of central and northern Germany. Coastal areas of the Netherlands, and western and northern UK also contained stations with high SE measurements. Additionally, mountainous areas of southern France and stations on the French island of Corse contained high SE measurements. For the peak gust wind speed models, high SE measurements were recorded in near-identical areas in mountainous and coastal regions with an additional station in Ireland reporting high SE measurements. Stations coinciding with the optimal model(s) based on SE measurements were also highlighted and continued to persist in mountainous and coastal areas.

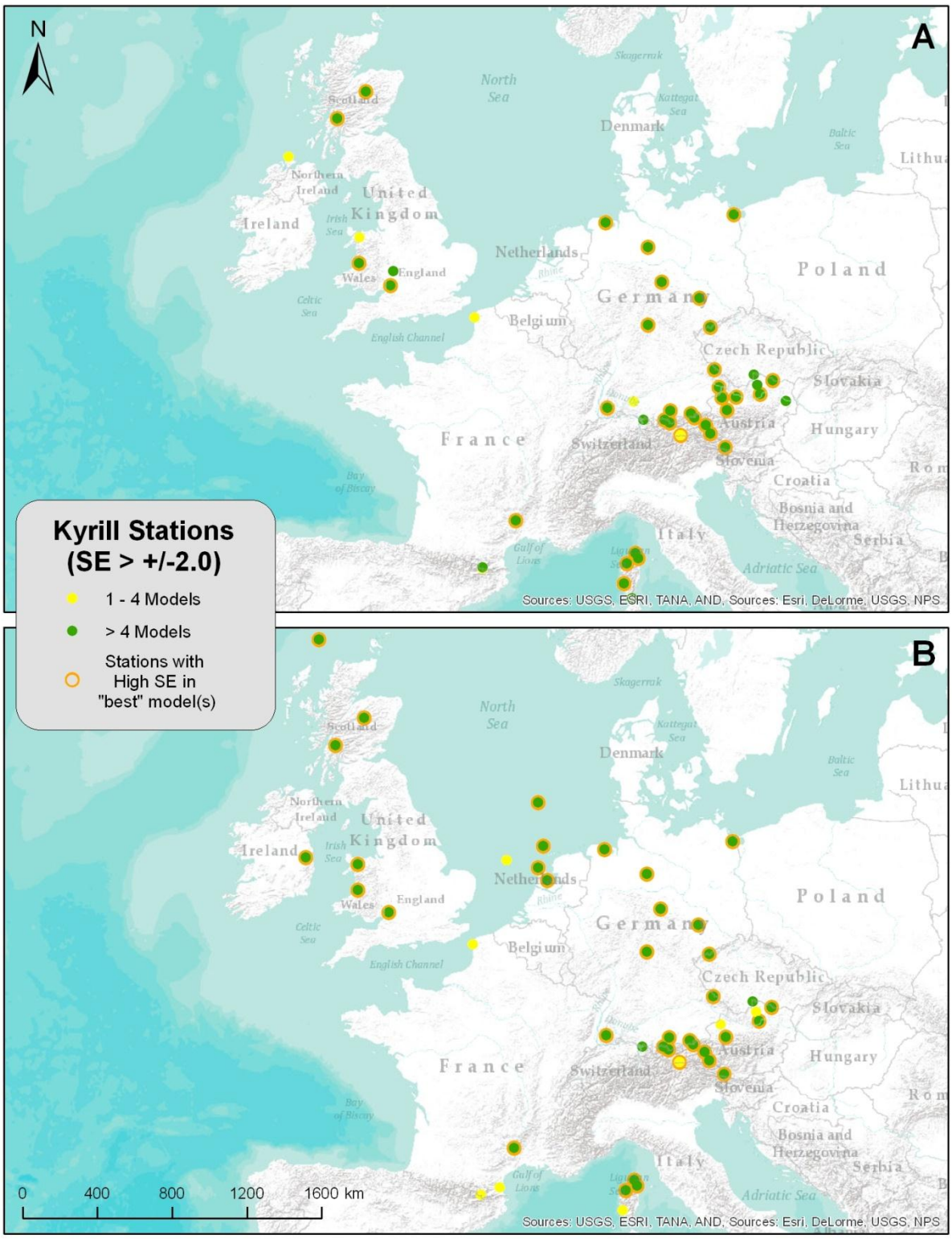

Figure 11. Locality of stations reporting high SE measurements for maximum sustained (A) and peak gust (B) winds.

3.2.4 Wind storm Paula

Wind storm Paula impacted much of northern Europe in January 2008 as it tracked across Norway, Sweden, Finland, and Denmark. Paula developed from a low pressure system in the North Atlantic Ocean and had a long, attached frontal boundary that impacted areas of Europe as far south as Austria. High winds were distributed over relatively large areas with some of the highest winds occurring in the Alps away from the center of circulation. The wind storm moved from west to east with major damage occurring in Scandinavia, Germany, Poland, and Austria. Only one death was reported, but ~€300 million (euros) in damage were attributable to Paula in Austria (Lloyds 2008, VRS 2008). During Paula, several wind observation stations in Norway, Germany, Poland, and Austria reported gust wind speeds in excess of 40 m s^{-1} – comparable to Category 2 hurricane wind speeds. Building roofs, communication and transport networks, power lines and trees were damaged by high wind speeds (VRS 2008).

While Paula impacted a large area, Austria was particularly hard-hit despite higher winds not being identified in the country by any models. The results of cokriging models for maximum sustained (Figure 12) and peak gust (Figure 13) wind speeds provided additional evidence of the general west-east storm track for Paula. Wind speeds approaching 36 m s^{-1} were estimated by multiple peak gust models in coastal western areas of the Norway. Peak gust wind speeds greater than 20 m s^{-1} persisted across Denmark, northeastern Germany, and some parts of western Poland. Some differences in wind speed estimates were observed between modeled surfaces. For example, Figures 12a, 12c, 13a, 13b, and 13c showed a pocket of higher winds around Copenhagen and another pocket in southwestern Poland, while other models estimated a gradual deterioration of wind speeds from west to east. Localized higher winds in Austria may have been smoothed by the global interpolation process, but could potentially be identified with regional wind speed models.

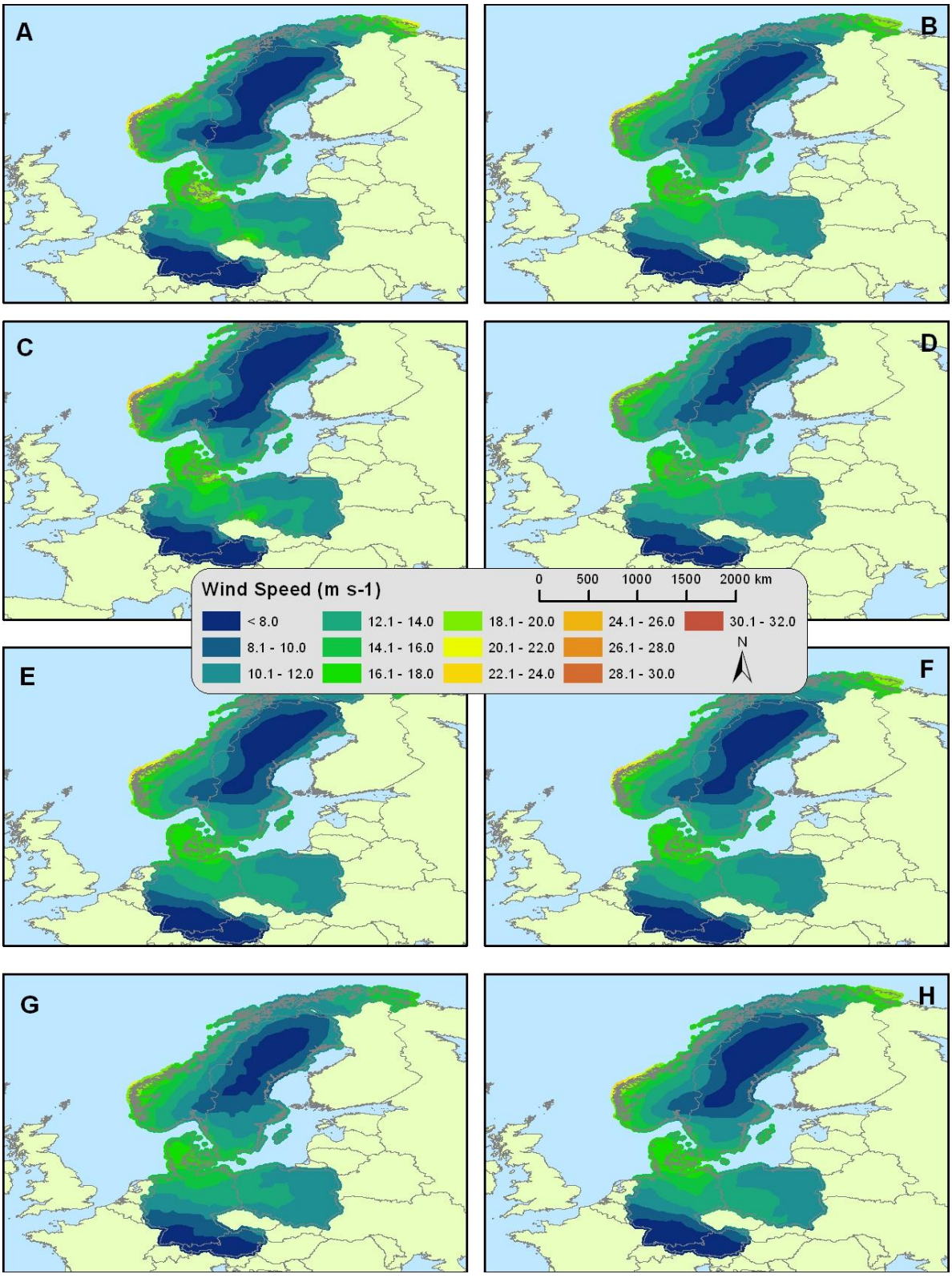

Figure 12. Maximum sustained wind surface estimates for wind storm Paula produced by the following models: original kriging (A), cokriging with elevation (B), cokriging with aspect (C), cokriging with land cover (D), cokriging with elevation and aspect (E), cokriging with elevation and land cover (F), cokriging with aspect and land cover (G), and cokriging with elevation, aspect, and land cover (H).

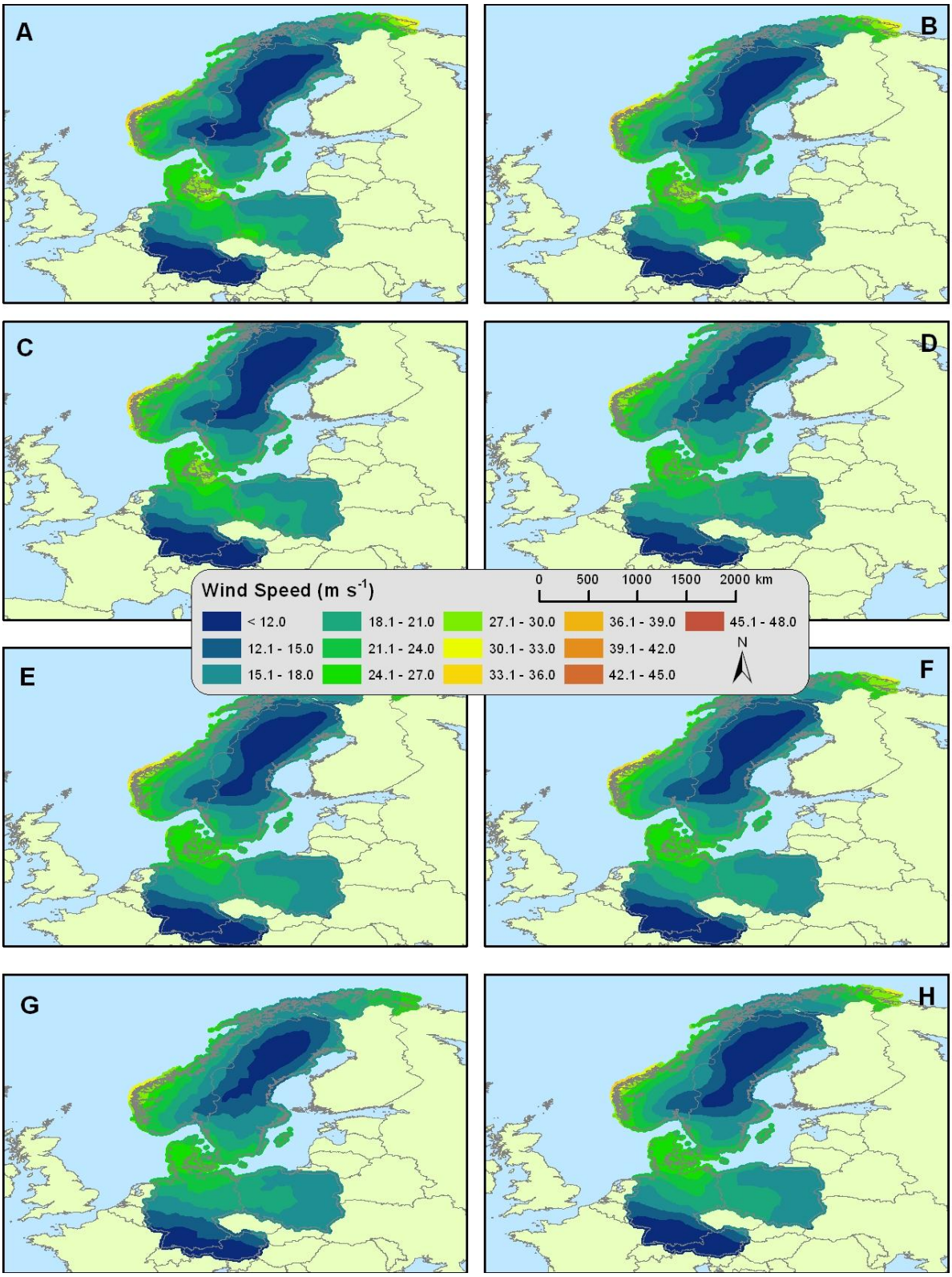

Figure 13. Peak gust wind surface estimates for wind storm Paula produced by the following models: original kriging (A), cokriging with elevation (B), cokriging with aspect (C), cokriging with land cover (D), cokriging with elevation and aspect (E), cokriging with elevation and land cover (F), cokriging with aspect and land cover (G), and cokriging with elevation, aspect, and land cover (H).

To determine the optimal model(s) for each wind speed type for wind storm Paula, multiple accuracy metrics were utilized during model implementation. The accuracy metrics for each model and wind type were aggregated in Table 10. For the wind storm Paula maximum sustained wind models, the original kriging methodology produced the automated anisotropic conditions closest to the actual storm track of ~100°. Four models produced the lowest RMSPE score of 4.49, while the ME score nearest to zero was produced by the original kriging model and the cokriging model utilizing aspect. The RMSE score nearest to one was produced by four cokriging models utilizing various combinations of all three covariates. Two models (cokriging with land cover and cokriging with aspect and land cover) reported the fewest number of stations (17) with high SE measurements after cross-validation. For the peak gust wind models, the original kriging methodology again produced the automated anisotropic conditions closest to the actual storm track of ~100°. Two models (cokriging with elevation and cokriging with aspect) produced the RMSE score nearest one and two different models (cokriging with land cover and cokriging with aspect and land cover) reported the fewest number of stations (18) with high SE measurement of greater than +/-2.0. The model utilizing elevation as a covariate received the lowest RMSPE score, while the ME nearest to zero was produced by the original kriging model.

Table 10. Wind storm Paula accuracy metrics.

Storm	Method	Anisotropy	RMSPE	ME	RMSE	SE (> +/- 2.0)
Paula	Original Kriging	86.3	4.49	0.002	1.06	39
Max	Cokriging w/elev	68.0	4.49	0.012	1.00	33
Sustained	Cokriging w/asp	52.7	4.50	0.002	1.03	33
	Cokriging w/LC	64.0	4.58	0.020	0.89	17
	Cokriging w/elev & asp	68.0	4.49	0.012	1.00	33
	Cokriging w/elev & LC	68.0	4.51	0.014	1.00	33
	Cokriging w/asp & LC	64.0	4.58	0.020	0.89	17
	Cokriging w/elev, asp, & LC	68.0	4.49	0.012	1.00	33
Paula	Original Kriging	86.1	7.09	0.002	1.07	38
Peak	Cokriging w/elev	69.1	7.05	0.012	1.00	40
Gust	Cokriging w/asp	44.8	7.15	0.006	1.00	30
	Cokriging w/LC	64.0	7.25	0.019	0.90	18
	Cokriging w/elev & asp	68.0	7.08	0.011	1.01	30
	Cokriging w/elev & LC	68.0	7.12	0.013	1.02	32
	Cokriging w/asp & LC	63.8	7.26	0.019	0.90	18
	Cokriging w/elev, asp, & LC	68.0	7.12	0.013	1.02	32

To examine in more detail the locations of stations where high SE measurements occurred, maps were produced for each wind type for wind storm Paula (Figure 14a-b). Most stations that received high SE measurements received such measurements from multiple models. For the maximum sustained wind speed models, high SE measurements were recorded by stations in the Alps of Austria, and southern Germany as well as coastal and interior stations in the southern half of Norway. Other stations receiving high SE measurements were scattered in coastal Sweden, Germany, and Poland as well as the rugged border between Germany and the Czech Republic. For the peak gust wind speed models, high SE measurements were recorded in near-identical areas in mountainous and coastal regions with a few exceptions. Stations coinciding with the optimal model(s) based on SE measurements were also highlighted and occurred in concomitant geographical areas.

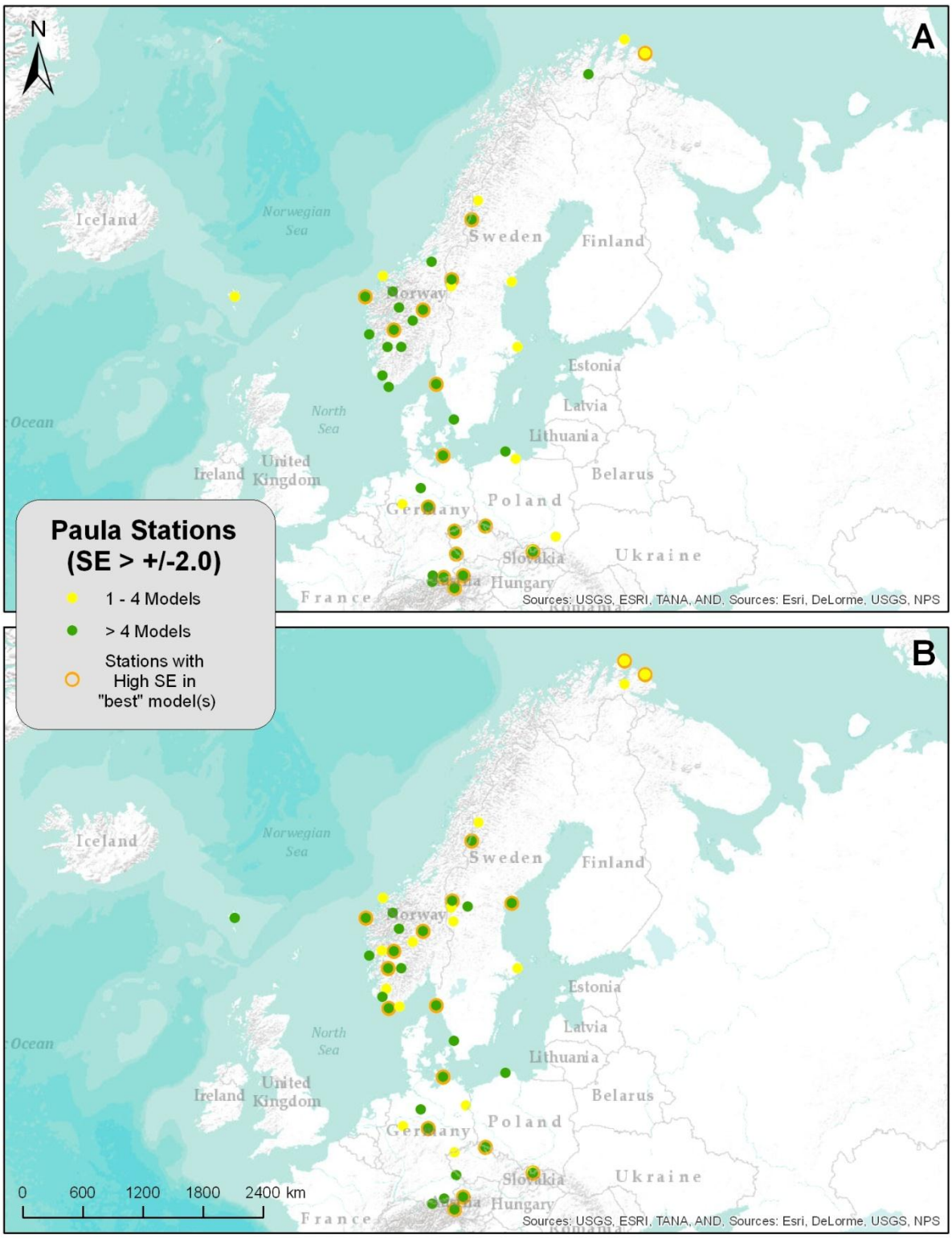

Figure 14. Locality of stations reporting high SE measurements for maximum sustained (A) and peak gust (B) winds.

3.2.5 Wind storm Emma

Wind storm Emma moved across northern and central Europe between 29 February and 1 March 2008 predominantly impacting the Netherlands, Belgium, Switzerland, Germany, Austria, Czech Republic, and Poland. Emma developed from a low pressure system in the North Atlantic Ocean and joined a separate frontal system as it tracked into northern Europe making it a very complex storm with disproportionately high sustained wind speeds and widely varying wind directions. The variance in wind directions created confusion during modeling when anisotropy was considered. The wind storm moved from west to east across northern Europe with the frontal boundary extending into southern Europe. Approximately 15 deaths and €1.3 billion (euros) in insured losses were attributable to Emma with almost €1 billion of damage in Germany and ~€200 million of damage in Austria alone (Guy Carpenter 2008). The biggest losses occurred in the Bavaria region of southeastern Germany. During Emma, several wind observation stations in Bavaria and Austria around Salzburg and Vienna reported gust wind speeds in excess of 35 m s^{-1} – comparable to Category 1 hurricane wind speeds. Building roofs, communication and transport networks, power lines, automobiles, and trees were particularly hard-hit by high wind speeds, while flooding was a major concern in many eastern European countries (Guy Carpenter 2008).

The results of cokriging models for maximum sustained (Figure 15) and peak gust (Figure 16) wind speeds provided additional evidence of the general west-east storm track for Emma, while also alluding to the northwest-southeast wind speeds associated with the initial frontal system. Wind speeds approaching 33 m s^{-1} were estimated by several peak gust models in near the Germany-Denmark border, while only one peak gust model (Figure 16e) indicated similar wind speeds in the Bavaria region of Germany near Austria as well as small areas of the Czech Republic. The highest sustained and peak gust wind speeds occurred in coastal areas of the Netherlands and Germany as well as interior southern areas of Germany, with a slight decrease in wind speeds evidenced in the northern plains of Germany. Some differences in wind speed estimates were observed between most surfaces. For example, Figures 15e, 15f, and 15g showed very spotty and localized high wind speeds that appeared to be influenced by topography since each of those models used elevation and/or aspect as covariates. The other, more smoothed surfaces may be more indicative of wind storm Emma's general wind speeds and patterns based on accuracy analysis – highlighting the complexity of surface winds caused by the unique meteorology associated with Emma.

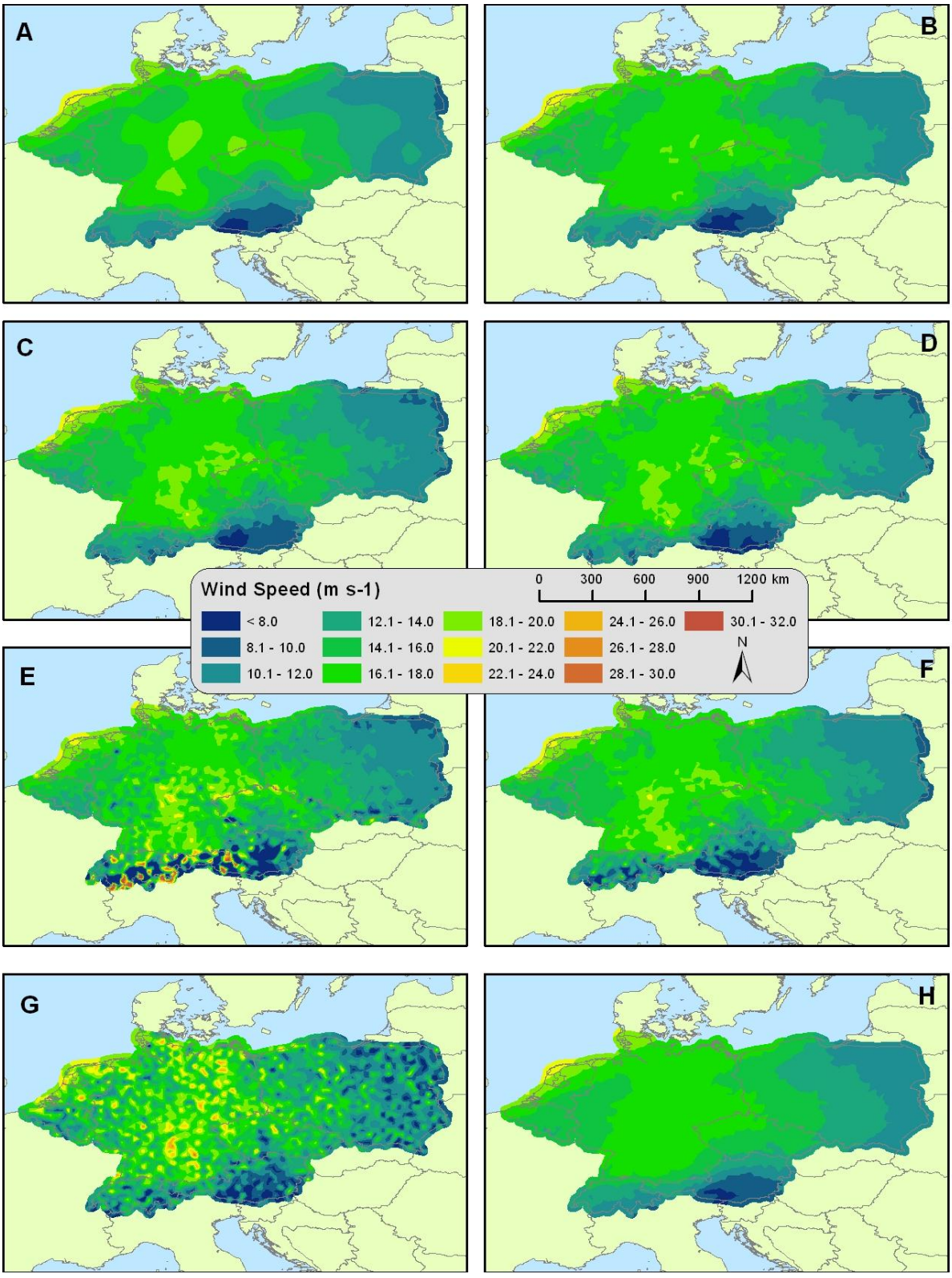

Figure 15. Maximum sustained wind surface estimates for wind storm Emma produced by the following models: original kriging (A), cokriging with elevation (B), cokriging with aspect (C), cokriging with land cover (D), cokriging with elevation and aspect (E), cokriging with elevation and land cover (F), cokriging with aspect and land cover (G), and cokriging with elevation, aspect, and land cover (H).

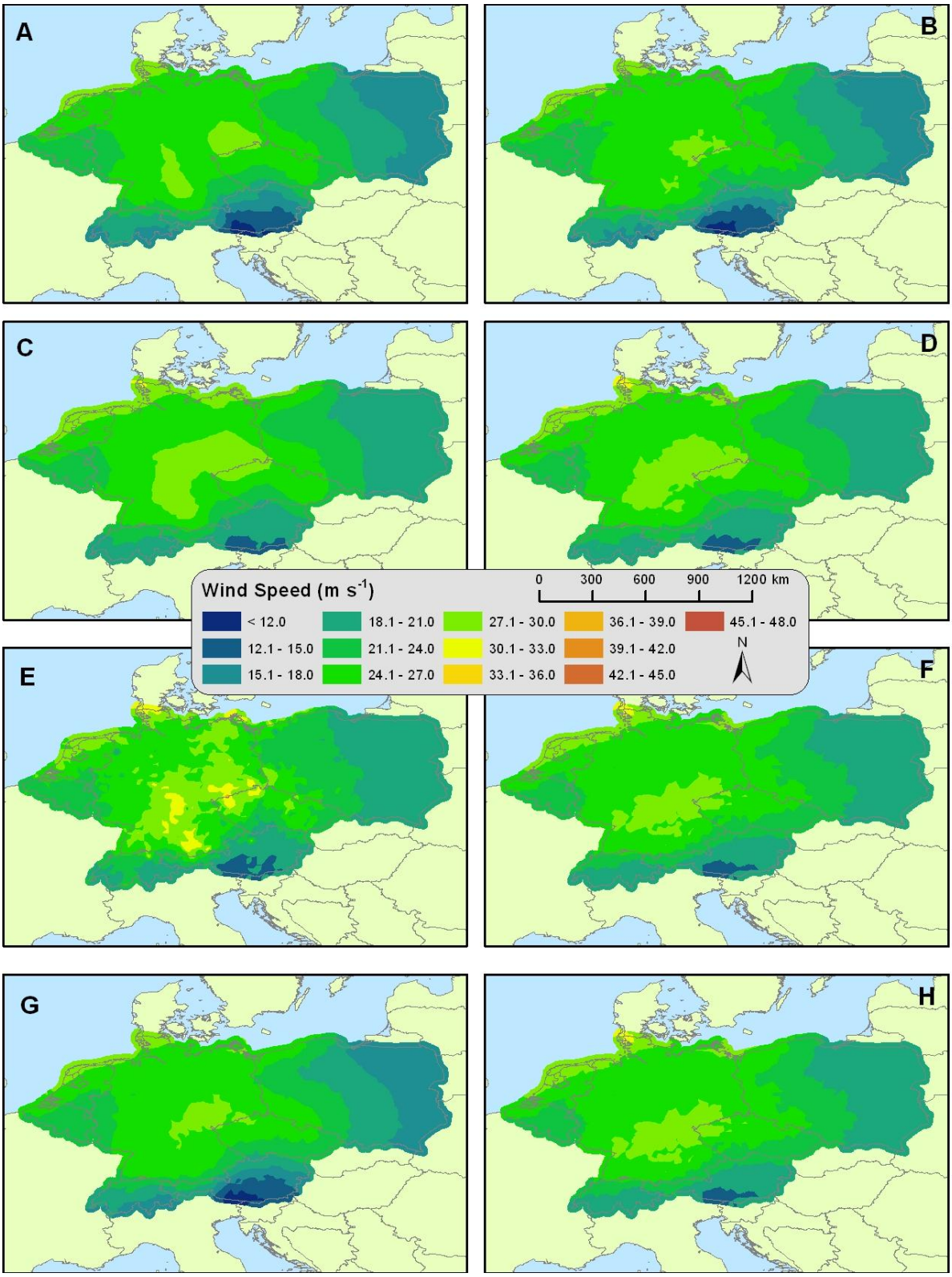

Figure 16. Peak gust wind surface estimates for wind storm Emma produced by the following models: original kriging (A), cokriging with elevation (B), cokriging with aspect (C), cokriging with land cover (D), cokriging with elevation and aspect (E), cokriging with elevation and land cover (F), cokriging with aspect and land cover (G), and cokriging with elevation, aspect, and land cover (H).

To determine the optimal model(s) for each wind speed type for wind storm Emma, multiple accuracy metrics were utilized during model implementation. The accuracy metrics for each model and wind type were aggregated in Table 11. For the wind storm Emma maximum sustained wind models, the cokriging methodology utilizing land cover produced the automated anisotropic conditions closest to the actual storm track of ~113°, but automated anisotropy differed greatly between models. The model utilizing the covariate elevation as well as the model utilizing all three covariates produced the lowest RMSPE score, while the ME nearest to zero and fewest stations with high SE measurements (12) was produced by the model utilizing only land cover. The combination of aspect and land cover produced the RMSE score nearest to one. For the peak gust wind models, the model utilizing only land cover and the model utilizing both aspect and land cover produced the automated anisotropic conditions closest to the actual storm track of ~113°. Multiple models produced the lowest RMSPE score, including the model utilizing only land cover as a covariate. Two models (elevation and land cover, all three covariates) were tied for the fewest stations (16) reporting a SE measurement of greater than +/-2.0. The model utilizing elevation as a covariate received the ME nearest to zero, while the RMSE nearest to one was produced by two models: the original kriging model and the model incorporating aspect and land cover.

Table 11. Wind storm Emma accuracy metrics.

Storm	Method	Anisotropy	RMSPE	ME	RMSE	SE (> +/- 2.0)
Emma	Original Kriging	58.4	5.05	0.002	0.96	20
Max	Cokriging w/elev	159.6	5.02	0.001	0.92	16
Sustained	Cokriging w/asp	1.8	5.16	-0.015	0.82	13
	Cokriging w/LC	71.0	5.16	0.000	0.81	12
	Cokriging w/elev & asp	17.6	10.54	0.130	1.97	91
	Cokriging w/elev & LC	0.0	6.11	0.004	0.94	24
	Cokriging w/asp & LC	3.9	6.26	0.011	1.02	27
	Cokriging w/elev, asp, & LC	68.0	5.02	0.005	0.91	16
Emma	Original Kriging	42.7	8.25	0.005	0.96	20
Peak	Cokriging w/elev	159.8	8.21	0.000	0.91	18
Gust	Cokriging w/asp	43.8	8.25	0.006	0.95	20
	Cokriging w/LC	154.3	8.21	0.002	0.94	21
	Cokriging w/elev & asp	16.5	15.99	0.111	1.81	84
	Cokriging w/elev & LC	68.0	8.21	0.003	0.89	16
	Cokriging w/asp & LC	154.3	8.21	0.029	0.94	21
	Cokriging w/elev, asp, & LC	68.0	8.21	0.003	0.89	16

To examine in more detail the locations of stations where high SE measurements occurred, maps were produced for each wind type for wind storm Emma (Figure 17a-b). Most stations that received high SE measurements received such measurements from multiple models. The major exceptions were the models that incorporated elevation and aspect collectively as covariates. These models reported a large number of stations with high SE measurements located predominantly in the Alps of Switzerland and Austria. For the maximum sustained wind speed models, most high SE measurements were recorded by stations in mountainous regions of Switzerland, Austria, and southern Germany as well as a rugged area in central Germany and mountainous border between the Czech Republic and Germany. Stations in coastal areas reported very few high SE measurements with only one station on the Baltic Sea coast of Poland reporting multiple high SE measurements. For the peak gust wind speed models, high SE measurements were recorded in near-identical areas in mountainous and rugged regions as well as the one coastal station in Poland. Stations coinciding with the optimal model(s) based on SE measurements were also highlighted and, while improved compared to other models, continued to indicate a complex and difficult-to-model environment in mountainous areas.

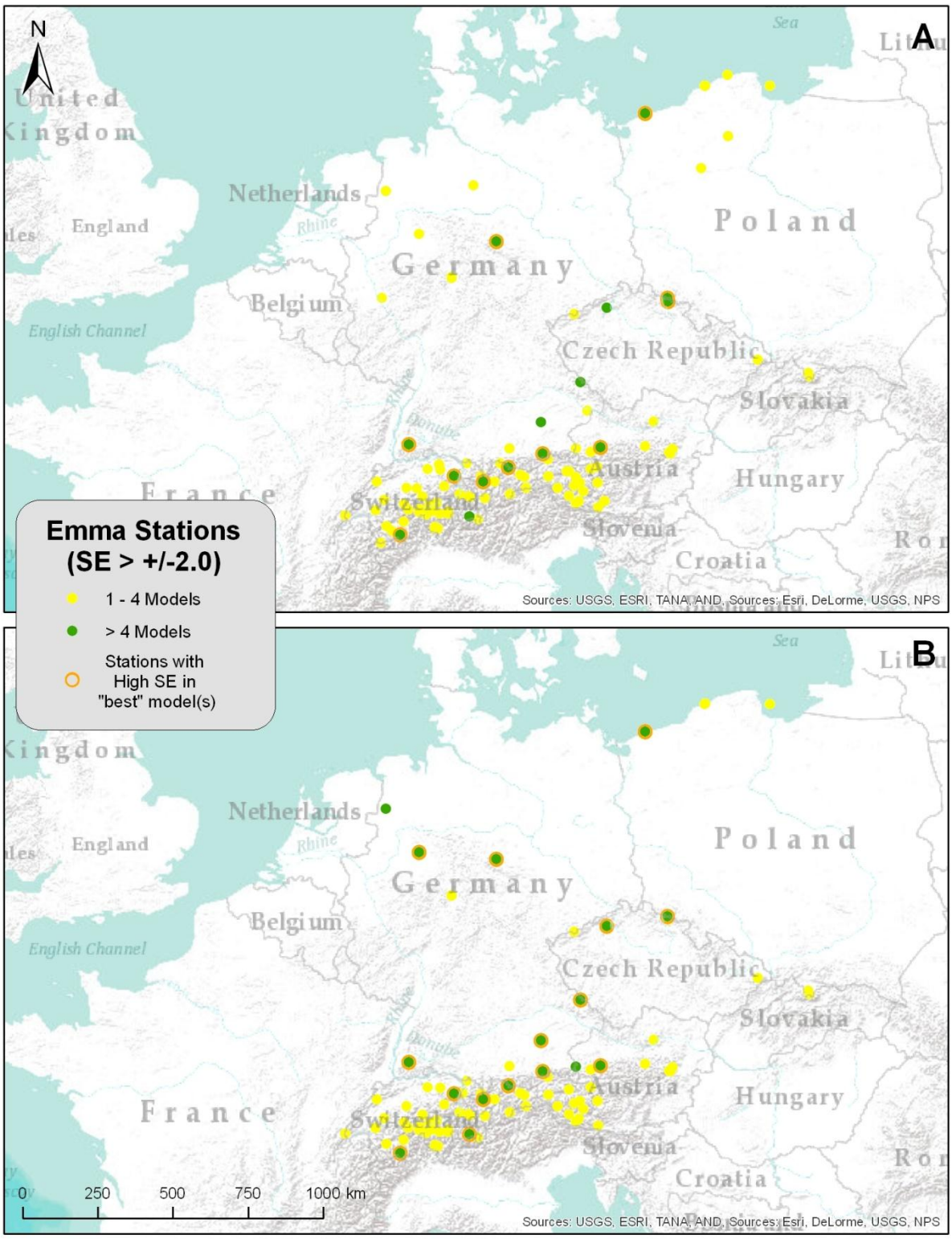

Figure 17. Locality of stations reporting high SE measurements for maximum sustained (A) and peak gust (B) winds.

4. Discussion

4.1 Optimizing surface wind estimates through cokriging

Seven different cokriging models were produced using singular and assimilated combinations of each covariate with varying results of modification compared to the results from the original kriging methodology. The original kriging model was also produced for each of the five storms to allow for a side-by-side visual and statistical comparison through the use of multiple accuracy metrics. Overall, 80 different modeled surface estimates were created – 16 for each of the five wind storms – and standard error maps were also created for each wind type. The maps showed that most models produced logical surface estimates based on the known track, wind speed, and wind direction associated with each storm. All wind storms followed a general west-east track across either central or northern Europe with the UK, France, the Netherlands, Belgium, and Germany being impacted the most by high winds and infrastructure damage. The highest winds associated with each storm occurred predominantly in coastal and mountainous areas with a common tendency for winds to subside slightly as they moved inland, then to increase again when approaching the mountainous regions. Higher levels of uncertainty (or error) were associated with both the coastal and mountainous regions. Wind speeds are difficult to model in coastal regions for two reasons: 1) the land-ocean interface creates turbulence and deflection when the surface that wind moves across changes (Wieringa 1973, 1986) and 2) wind observation stations rarely exist over water, thus providing an abrupt departure in station density (MacEachren and Davidson 1987, Wieringa 1997). Wind speeds are difficult to model in mountainous regions for two reasons as well: 1) wind is deflected and funneled in multiple directions by varying topography (Wieringa 1973, 1986) and 2) as winds move upslope and downslope, wind speed also changes resulting in locally high/low winds (Bowen and Lindley 1977, Hertenstein and Kuettner 2005). These local wind patterns are difficult to estimate using a global model.

Figures 15e and 15g (wind storm Emma) provide an example of global wind surfaces that were too specific in assigning local wind patterns and created a surface where the general wind patterns were difficult to visualize. These same models also produced higher station error relative to the original kriging surface. Because Emma was a complex storm that coincided with a separate frontal system moving across Europe, some model uncertainly may be expected. Wind direction was also very difficult to model for Emma because of the contrasting atmospheric systems. Excluding the models from Figures 15e and 15g, the use of covariates most often improves upon the original kriging surface by reducing station error.

Covariates were not significantly spatially autocorrelated, but wind speed was autocorrelated and the use of anisotropy during modeling helped in identifying overall trends in wind direction based on high/low wind speeds. Most modeled surfaces illustrated the general west-east or northwest-southeast movement of each wind storm, but the azimuth directions identified by the automatic anisotropy process sometimes varied widely. For example, azimuth direction varied by as much as ~35° for the models produced for wind storm Emma. The highest disparity was observed between the original kriging surfaces and the model that used only aspect as a covariate. This may indicate that the addition of aspect resulted in a more nuanced wind surface that possibly contained multiple wind directions at specific locations where one side of a mountain may have deflected the wind in a way that was different from the general wind pattern. Topography can deflect wind and create changes in turbulence in the area immediately behind a mountain or mountain range (Bowen and Lindley 1977).

Accuracy metrics were highly varied, indicating that one singular covariate does not always improve wind surface estimates for wind storms over large, heterogeneous terrain. However, the major index of standard error (SE) reduction showed improvement over the original kriging surface in eight out of the ten model sets, with only one set (peak gust models for wind storm Kyrill) indicating that original kriging was optimal. Several peak gust models for wind storm Lothar did not reduce the SE, but also did not increase the SE. The original kriging method also reported the lowest SE measurement in the set of peak gust models for wind storm Lothar, but five other models reported the identical stations with high SE (16) as well. The SE for wind storm Paula was reduced by more than half (Table 10) and provided an example of how a singular covariate (land cover in this case) made a major improvement in surface estimates. Overall, the model output of the optimal version was greatly improved compared to the original kriging model similar to previous research (Luo et al. 2008, Akkala et al. 2010, Zlatev et al. 2010, Luo et al. 2011).

Overall, models utilizing land cover (singularly or in conjunction with elevation and/or aspect) tended to produce optimal wind speed surface estimates. This was not always true. The optimal maximum sustained wind speed model for wind storm Kyrill was produced using only aspect as a covariate, while the optimal peak gust wind speed model for wind storm Jeanette was produced using both elevation and aspect collectively. Additionally, models utilizing land cover were much more computational intensive typically taking several hours (and occasionally days with larger areas, i.e., wind storm Jeanette), while models utilizing elevation and/or aspect were completed in less than one hour. This was most likely due to the

complex nature of actual land cover on the surface as well as the categorical nature of the dataset within the geostatistical modeling environment. Each step of the process was conducted manually resulting in a more complicated and extended modeling process that would have been improved through automation. Regardless of modeling complexity and intensiveness, the general improvement shown by models utilizing land cover is promising for future modeling efforts and covariate creation.

4.2 Overall impact of improved wind surface estimates

Improved wind surface estimates created through cokriging build on previous research that only utilized one covariate (elevation) to model wind speeds. The addition of aspect and land cover improved surface estimates and may be used for other wind- or even non wind-related research. The use of other covarites within cokriging may help to address other problems, ranging from hazards to energy. Within wind storm research, models and extreme-event climatologies of wind simulation and hazard/risk assessment that are widely used in the insurance/reinsurance industry can be improved through the incorporation of our research results. This study may also help to inform local cost-benefit studies and subsequently save lives and resources for local government, private industry, and consumers. Damage estimates may also be refined based on the resulting wind surface estimates, thus improving construction standards and adapting insurance needs. The known impacts of wind storms on vegetation (*e.g.*, trees; Kirk and Franklin 1992) and civil infrastructure (Reed 2008) are severe, and improved spatial interpolations for wind storm-induced wind speeds will be fundamental to evaluating damages as well as potential changes needed for forest management and building codes/regulations. The identification of high wind zones will also help to inform local government vulnerability assessments that may be included in future hazard mitigation plans. The results may also improve understanding of common wind storm features (*e.g.*, directions, wind movements/patterns, surface interactions, etc.) that have long-term, but not necessarily immediate, impacts on sectors such as transportation, agriculture, and recreation.

5. Future Research

Local cokriging surfaces (*e.g.*, country- and state-level) will be the focus of future research and these surfaces will be created to examine more specific wind speeds and directions that are often smoothed when performing regional cokriging (*e.g.*, all of Europe). This smoothing was evident in each of ten model sets because the general wind direction and

speed were mapped correctly, but local high wind speeds were more difficult to discern. Damage data (e.g., trees, infrastructure) may also be joined and overlaid spatially with the optimal local wind surface estimates to establish a damage-wind ratio. An example of local kriging/cokriging and damage overlay are examined in the subsequent section (5.1). Proximity analysis and exposure-testing using aspect and slope may further aid in understanding high damage locations associated with wind storms. High wind speeds will likely recur in similar areas, thus there is also a need to identify repetitive high wind and high damage environments. Using the ideal cokriging parameters and covariate combinations identified for Europe in this study, the transferability of the methods may also be tested for various wind storms in the Pacific Northwest region of North America where similar wind storms (called winter storms locally) occur. Successful transferability of cokriging methods would imply that the techniques are responsive to areas with differing terrains and land covers and that the methods are adaptable.

A major area of future research involves a complete remaking of the covariate dataset. While the cokriging interpolation method improved surface wind estimates, an additional procedure could be tested to reduce the inherent concern of autocorrelation between covariates. Just as principal components analysis (PCA) is used to combine strongly correlated variables into various components, a data reduction technique may be applied to create a "ruggedness" variable. Issues of autocorrelation could potentially be eliminated through the development of one variable that incorporates both elevation and land cover to represent terrain ruggedness. An anisotropic cokriging model will likely improve prediction of the contrasting effects on wind speeds caused by rough-to-smooth *vs*. smooth-to-rough terrain transition areas where ruggedness may change abruptly. The application of only one covariate may also help to reduce the error associated with the use of multiple covariates.

5.1 Wind storm Paula: an in-depth look at damages and winds in Austria

Winds from wind storm Paula were particularly damaging in Austria and warrant a closer examination utilizing local and more specific models as well as regional damage estimates. Wind storm-induced tree/infrastructure damage data have been obtained from Federal Ministry of Agriculture, Forestry, Environment, & Water Management (FMAFEWM) in Austria (http://www.lebensministerium.at/). These data include maps and imagery showing major forest damage in the Austrian states of Carinthia and Styria as well as point and polygon shapefiles that contain detailed information about impacted areas in hectares (ha) and in forestry management units (fm). Additional wind speed surfaces were obtained from the

Zentralanstalt fur Meteorologie und Geodynamik (ZAMG) (http://www.zamg.ac.at/cms/de/aktuell), which utilizes a different spatial weighting method for producing wind storm wind surface estimates.

Local cokriging surfaces (*e.g.*, country- and state-level) were created utilizing land cover as a covariate to examine more specific wind speeds and directions that are often smoothed when performing regional cokriging (*e.g.*, Figures 12 and 13). Collectively, the damage data and ZAMG wind surfaces were overlaid spatially with the optimal local wind surface estimates to determine if damages and high winds occurred in similar areas. In Figure 18, the original kriging algorithm was used to produce a local maximum sustained (18A) and peak gust (18B) wind surface estimate for Austria, while the cokriging method was utilized to produce the same surface estimates (18C and D) for comparison. All four surface estimates identified a large area of high wind in northeastern Austria in an area that is less mountainous than central and western Austria. In three out of the four models, small pockets of high wind also occurred along the Kärnten, Salzburg, and Tirol borders as well as the Steiermark and Oberösterreich borders. There were even smaller pockets of high wind scattered throughout other parts of the country. Table 12 shows the accuracy metrics for each map. The cokriging method produced the optimal maximum sustained wind speed model, while the original kriging method produced the optimal peak gust wind speed model based on the various metrics. The cokriging model for peak gust wind speed (Figure 18D) also appears highly fragmented indicating a poor fit.

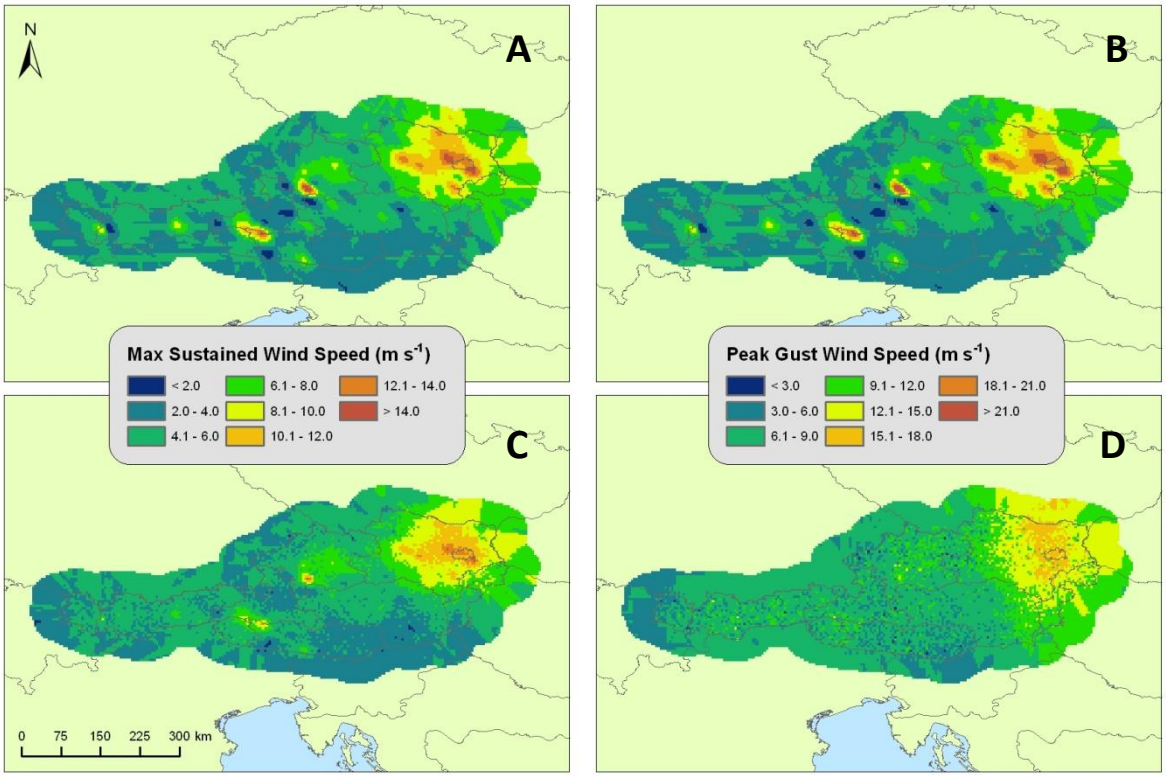

Figure 18. Original kriging models for maximum sustained (A) and peak gust (B) wind speeds and cokriging models for maximum sustained (C) and peak gust (D) wind speeds.

Table 12. Accuracy metrics for local kriging/cokriging models in Austria

Wind Type	Method	Anisotropy	RMSPE	ME	RMSE	SE (> +/- 2.0)
Maximum	Original Kriging	123.2	3.68	-0.02	0.87	3
Sustained	Cokriging w/LC	123.0	3.62	-0.02	0.87	2
Peak	Original Kriging	122.0	5.92	-0.01	0.88	4
Gust	Cokriging w/LC	178.1	6.00	0.00	0.99	5

Forestry damage data in Kärnten and Steiermark were overlaid on two separate wind speed maps: one produced by ZAMG and one produced by the local kriging peak gust model from Figure 18B. Forestry damage seemed to follow an invisible line from west to east across northern Kärnten and then a southwest-northeast line in Steiermark. Higher wind speeds were noticeable in the ZAMG wind surface map for most areas of Steiermark where forestry damage occurred, but higher wind speeds from the kriging surface were not omnipresent in all areas where forestry damage occurred. Specifically, the southernmost area of the largest block of forestry damage in Steiermark does not align with high wind surface estimates in the local kriging surface. In Kärnten, forestry damage did not always occur in areas of the highest wind speed as estimated by either wind estimate surface, but instead may have been

more dictated by other variables individually. Since damage estimates were provided at point (longitude, latitude) locations for Kärnten, values for elevation, land cover, and aspect were extracted for each location and visualized in Figures 20, 21, and 22. For most damage locations, elevation ranged between 750 and 1,750 meters (Figure 20). Dense needle-leaved evergreen land cover dominated areas where forestry damage was high (over 60% of damage), indicating that areas with this vegetation type are more susceptible to wind damage than other vegetation types (Figure 21). Wind storm Paula tracked from east to west and most wind speed directions indicated a northwest-southeast wind during the most intense segment of the storm, but the majority of forestry damage occurred on slopes that were either north/northeast-facing or south/southwest-facing (Figure 22). This may infer that wind speed from a slight (45°+) angle could be the most damaging during a wind storm. Figure 22 also clearly illustrates the increase in wind speed upslope AND downslope during a wind storm. For this reason, aspect may have added a conflicting element to cokriging models for wind storm Paula since winds often change directions, deflect off of mountains, and funnel through valleys resulting in less favorable accuracy metrics than the top models (original kriging and cokriging with land cover). Aerial images showing forestry damage inflicted by wind storm Paula can be viewed in Figure 23.

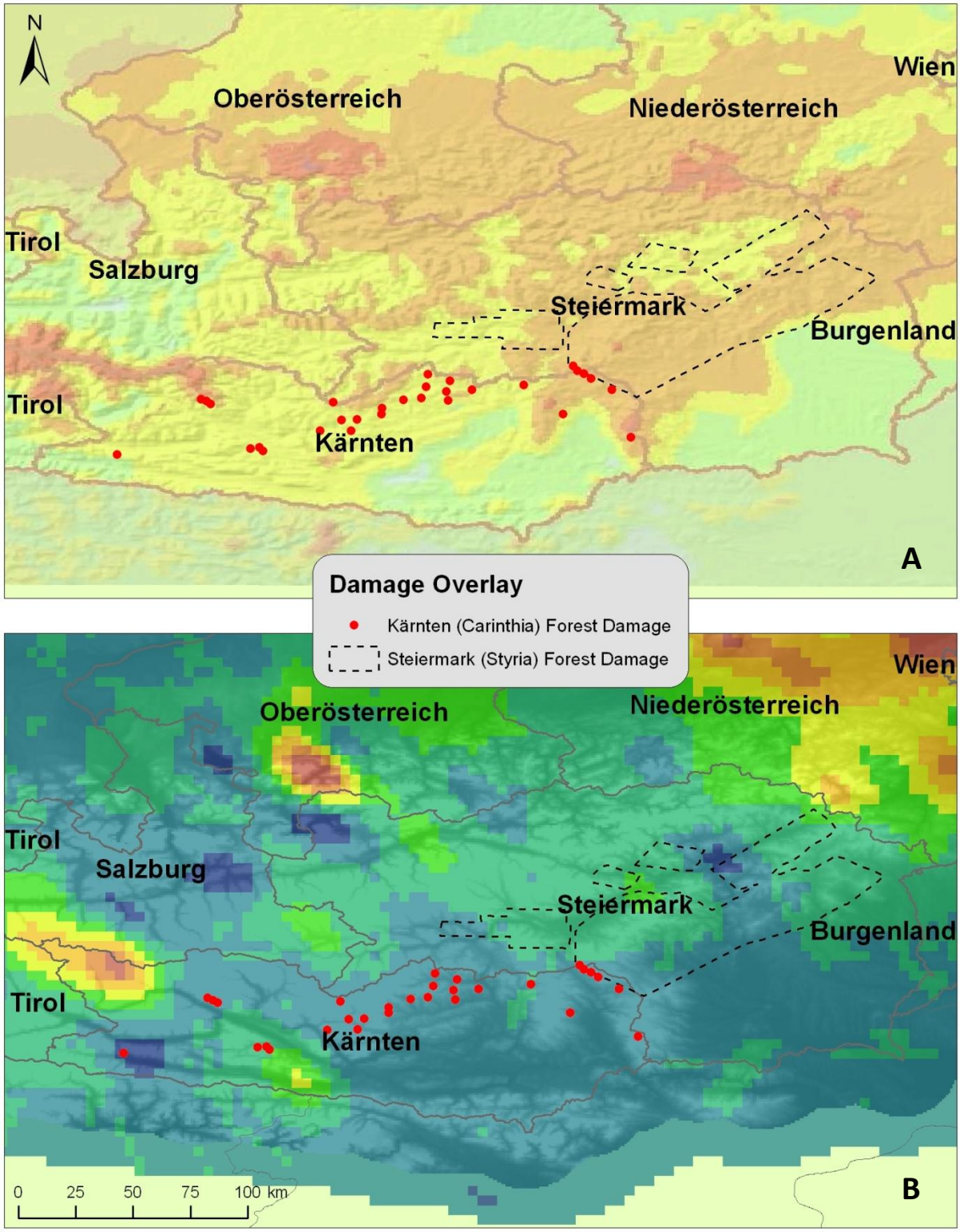

Figure 19. Wind surface estimates from ZAMG (A) and local kriging (B) overlaid with forestry damage locations.

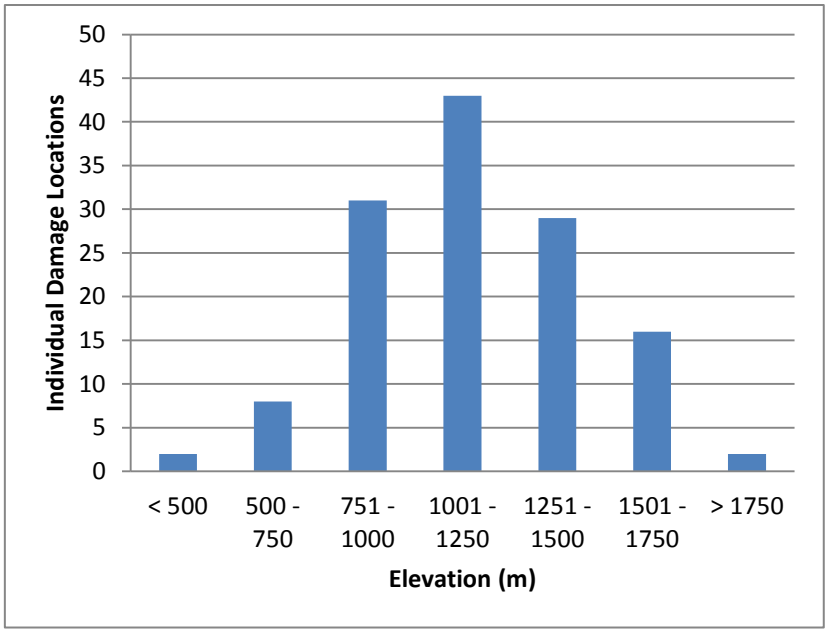

Figure 20. Distribution of elevation at each location where forestry damage was reported.

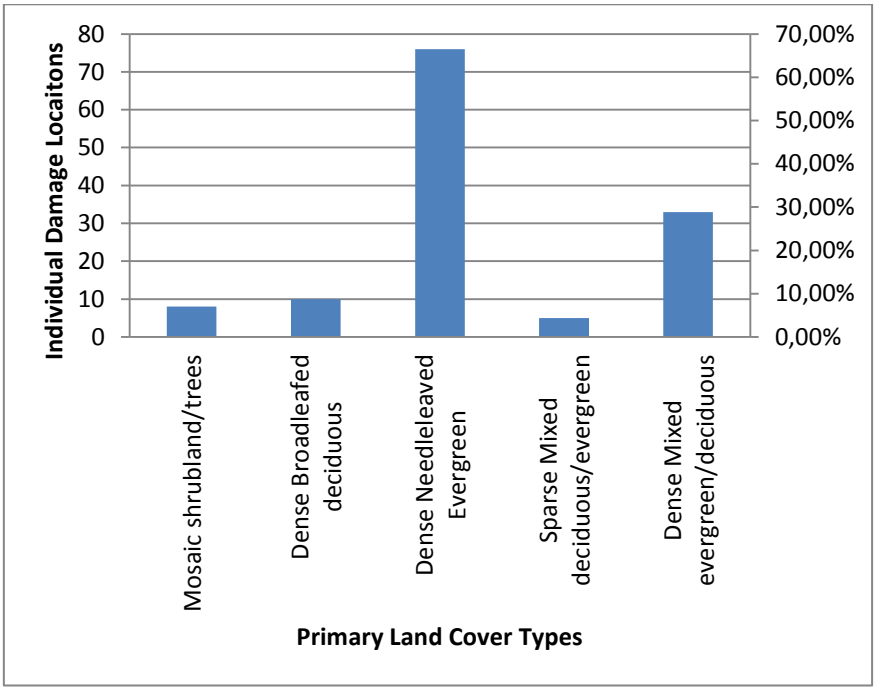

Figure 21. Distribution of primary land cover types at each location where forestry damage was reported.

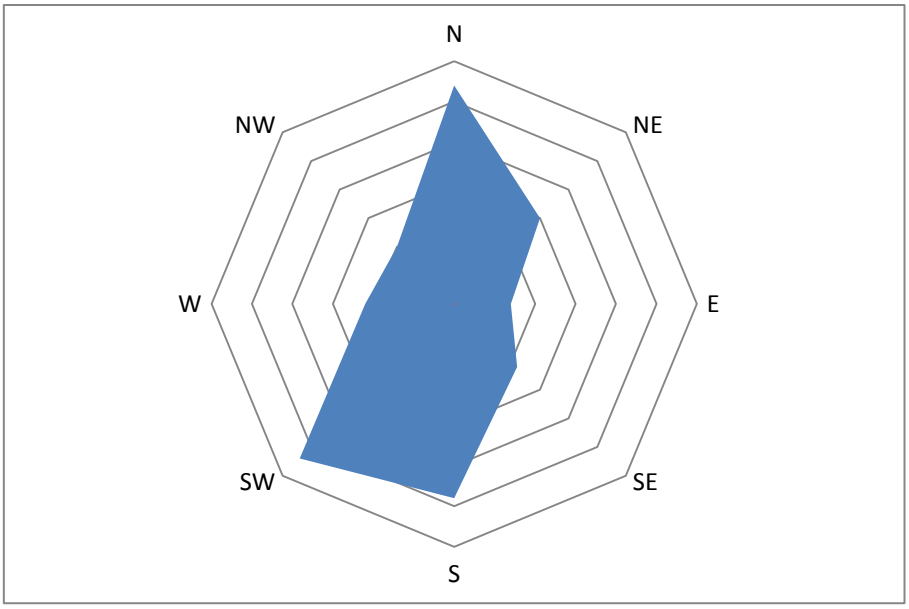

Figure 22. Aspect of topography at each location where forestry damage was reported.

Figure 23. Aerial images where forestry damage occurred during wind storm Paula.

6. Conclusions

Cokriging was utilized to create maximum sustained and peak gust wind speed surface estimates for five European wind storms over a 10-year period. The results confirmed that cokriging is superior to kriging for most models and that elevation is a good covariate. The study expanded on the use of covariates by adding aspect and land cover, which also showed improvement in most models from previous kriging models. Maps showing stations with high SE were also produced and indicated that some stations were repeatedly found to have high SE measurements. The major findings of this study include:

1) Aspect and land cover can be effective when used as covariates during the cokriging process.
2) In most model sets, the use of land cover as a covariate produced the best surface estimates with the fewest stations receiving high SE measurements.
3) Stations with high SE measurements continued to occur in coastal and mountainous regions, but were reduced by cokriging in most model sets.
4) General wind speed and wind direction patterns were modeled correctly at a global scale, but more localized patterns were not identified.
5) The use of multiple covariates resulted in variability when identifying the dominant azimuth direction of wind associated with each storm.

References

Akkala, A., V. Devabhaktuni, and A. Kumar. 2010. Interpolation techniques and associated software for environmental data. Environmental Progress & Sustainable Energy **29**:134-141.

ASCE 7-10. 2010. Wind Loads - General Requirements: Figure c26.5-1.

Atkinson, P. M., E. Pardo-Iguzquiza, and M. Chica-Olmo. 2008. Downscaling Cokriging for Super-Resolution Mapping of Continua in Remotely Sensed Images. Geoscience and Remote Sensing, IEEE Transactions on **46**:573-580.

Aznar, J. C., E. Gloaguen, D. Tapsoba, S. Hachem, D. Caya, and Y. Bégin. 2012. Interpolation of monthly mean temperatures using cokriging in spherical coordinates. International Journal of Climatology:n/a-n/a.

Bentamy, A., Y. Quilfen, F. Gohin, N. Grima, M. Lenaour, and J. Servain. 1996. Determination and validation of average wind fields from ERS-1 scatterometer measurements. International Publishers Distributor, Newark, NJ, ETATS-UNIS.

Bowen, A. J. and D. Lindley. 1977. A wind-tunnel investigation of the wind speed and turbulence characteristics close to the ground over various escarpment shapes. Boundary-Layer Meteorology **12**:259-271.

Cellura, M., G. Cirrincione, A. Marvuglia, and A. Miraoui. 2008. Wind speed spatial estimation for energy planning in Sicily: A neural kriging application. Renewable Energy **33**:1251-1266.

CGIAR-CSI. SRTM 90m Digital Elevation Data version 4: http://srtm.csi.cgiar.org/ Last accessed 7 January 2012.

Cook, N. J. 1986. Designers guide to wind loading of building structures. Part 1.

Cressie, N. 1986. Kriging nonstationary data. American Statistical Association, Alexandria, VA, ETATS-UNIS.

Cressie, N. 1990. The origins of kriging. Mathematical Geology **22**:239-252.

Della-Marta, P. M., H. Mathis, C. Frei, M. A. Liniger, J. Kleinn, and C. Appenzeller. 2009. The return period of wind storms over Europe. International Journal of Climatology **29**:437-459.

Donat, M. G., G. C. Leckebusch, S. Wild, and U. Ulbrich. 2011. Future changes in European winter storm losses and extreme wind speeds inferred from GCM and RCM multi-model simulations. Natural Hazards and Earth System Sciences **11**:1351-1370.

Dorland, C., R. S. J. Tol, and J. P. Palutikof. 1999. Vulnerability of the Netherlands and Northwest Europe to Storm Damage under Climate Change. Climatic Change **43**:513-535.

Durst, C. 1960. Wind speeds over short periods of time. Meteorological Magazine **89**:181-187.

EQE. 2000. The European Storms Lothar and Martin, December 26-28, 1999. ABS Consulting.

EQECAT. 2002. Report into the Storm "Jeanette," 27th October, 2002.

EQECAT. 2007. Europe Windstorm Kyrill Causes Losses in Western Europe.

ESRI. 2010. Earth Systems Research Lab: ArcGIS 10.0. Redlands, CA.

GlobCover. 2008. GlobCover Land Cover v2 2008 database. European Space Agency (ESA) GlobCover Project, led by MEDIAS-France. http://ionia1.esrin.esa.int/index.asp Last accessed 7 January 2012.

Guy Carpenter. 2008. Windstorm Emma.

Handorf, D. and K. Dethloff. 2009. Atmospheric teleconnections and flow regimes under future climate projections. The European Physical Journal - Special Topics **174**:237-255.

Helterbrand, J. and N. Cressie. 1994. Universal cokriging under intrinsic coregionalization. Mathematical Geology **26**:205-226.

Heneka, P. and T. Hofherr. 2011. Probabilistic winter storm risk assessment for residential buildings in Germany. Natural Hazards **56**:815-831.

Hertenstein, R. F. and J. P. Kuettner. 2005. Rotor types associated with steep lee topography: influence of the wind profile. Tellus A **57**:117-135.

Hewston, R. 2007. Windstorm Kyrill.*in* U. o. E. A.-. Norwich, editor.

Hofherr, T. and M. Kunz. 2010. Extreme wind climatology of winter storms in Germany. Climate Research **41**:105-123.

Joyner, T. A., A. M. Treviño, C. J. Friedland, S. Gosh, C. Huyck, and M. Weatherhead. *in review*. Peak gust and maximum sustained wind speed estimates for European mid-latitude cyclones. (Submitted to International Journal of Climatology).

Kirk, R. and J. Franklin. 1992. The Olympic rain forest: an ecological web. University of Washington Press, Seattle, Washington, USA.

Klawa, M. and U. Ulbrich. 2003. A model for the estimation of storm losses and the identification of severe winter storms in Germany. Natural Hazards and Earth System Sciences **3**:725–732.

Krayer, W. R. and R. D. Marshall. 1992. Gust factors applied to hurricane winds. Bulletin of the American Meteorological Society **73**:613-617.

Lanza, L., J. Ramirez, and E. Todini. 2001. Stochastic rainfall interpolation and downscaling. Hydrology and Earth System Sciences **5**:139-143.

Larsen, X. L. G. and J. Mann. 2006. The effects of disjunct sampling and averaging time on maximum mean wind speeds. Journal of Wind Engineering and Industrial Aerodynamics **94**:581-602.

Leckebusch, G. C., U. Ulbrich, L. Frohlich, and J. G. Pinto. 2007. Property loss potentials for European midlatitude storms in a changing climate. Geophysical Research Letters **34**.

Li, L., J. Wu, M. Wilhelm, and B. Ritz. 2012. Use of generalized additive models and cokriging of spatial residuals to improve land-use regression estimates of nitrogen oxides in Southern California. Atmospheric Environment **55**:220-228.

Lloyds. 2008. Exploring Europe's Double Whammy Windstorms. News & Features. Society of Lloyd's.

Luo, W., M. C. Taylor, and S. R. Parker. 2008. A comparison of spatial interpolation methods to estimate continuous wind speed surfaces using irregularly distributed data from England and Wales. International Journal of Climatology **28**:947-959.

Luo, X., Y. Xu, and Y. Shi. 2011. Comparison of interpolation methods for spatial precipitation under diverse orographic effects. Pages 1-5 *in* Geoinformatics, 2011 19th International Conference on.

MacEachren, A. and J. Davidson. 1987. Sampling and isometric mapping of continuous geographic surfaces. The American Cartographer **14**:299-320.

Mahdian, M. H., S. R. Bandarabady, R. Sokouti, and Y. N. Banis. 2009. Appraisal of the Geostatistical Methods to Estimate Monthly and Annual Temperature. Asian Network for Scientific Information, Pakistan.

Odeh, I. O. A., A. B. McBratney, and D. J. Chittleborough. 1995. Further results on prediction of soil properties from terrain attributes: heterotopic cokriging and regression-kriging. Geoderma **67**:215-226.

Öztopal, A. 2006. Artificial neural network approach to spatial estimation of wind velocity data. Energy Conversion and Management **47**:395-406.

Pardo-Iguzquiza, E., V. F. Rodríguez-Galiano, M. Chica-Olmo, and P. M. Atkinson. 2011. Image fusion by spatially adaptive filtering using downscaling cokriging. ISPRS Journal of Photogrammetry and Remote Sensing **66**:337-346.

Phillips, D. L., E. H. Lee, A. A. Herstrom, W. E. Hogsett, and D. T. Tingey. 1997. Use of auxillary data for spatial interpolation of ozone exposure in southeastern forests. Environmetrics **8**:43-61.

Pinto, J. G., C. P. Neuhaus, G. C. Leckebusch, M. Reyers, and M. Kerschgens. 2010. Estimation of wind storm impacts over Western Germany under future climate conditions using a statistical–dynamical downscaling approach. Tellus A **62**:188-201.

Raible, C. C. 2007. On the relation between extremes of midlatitude cyclones and the atmospheric circulation using ERA40. Geophysical Research Letters **34**:L07703.

Reed, D. 2008. Electric utility distribution analysis for extreme winds. Journal of Wind Engineering and Industrial Aerodynamics **96**:123-140.

RMS. 2002. RMS Updates Loss Estimates for Windstorm Jeanette; Insured Losses Likely to Exceed Euro 800 Million.

Schiermeier, Q. 2006. Insurers' disaster files suggest climate is culprit. Nature **441**:674-675.

Schmith, T., E. Kaas, and T. S. Li. 1998. Northeast Atlantic winter storminess 1875-1995 re-analysed. Climate Dynamics **14**:529-536.

Singh, V., C. Carnevale, G. Finzi, E. Pisoni, and M. Volta. 2011. A cokriging based approach to reconstruct air pollution maps, processing measurement station concentrations and deterministic model simulations. Environmental Modelling & Software **26**:778-786.

Sliz-Szkliniarz, B. and J. Vogt. 2011. GIS-based approach for the evaluation of wind energy potential: A case study for the Kujawsko–Pomorskie Voivodeship. Renewable and Sustainable Energy Reviews **15**:1696-1707.

Solari, G. 1993. Gust buffetting 1. Peak wind velocity and equivalent pressure. Journal of Structural Engineering-Asce **119**:365-382.

Sterk, G. and A. Stein. 1997. Mapping wind-blown mass transport by modeling variability in space and time. Soil Sci. Soc. Am. J. **61**:232-239.

Tobler, W. R. 1970. A Computer Movie Simulating Urban Growth in the Detroit Region. Economic Geography **46**:234-240.

Vauclin, M., S. R. Vieira, G. Vachaud, and D. R. Nielsen. 1983. The Use of Cokriging with Limited Field Soil Observations1. Soil Sci. Soc. Am. J. **47**:175-184.

Venäläinen, A. and M. Heikinheimo. 2002. Meteorological data for agricultural applications. Physics and Chemistry of the Earth, Parts A/B/C **27**:1045-1050.

VRS. 2008. Windstorm "Paula": damage of millions of euros.

Wahba, G. 1981. Spline interpolation and smoothing on the sphere. SIAM Journal of Scientific and Statistical Computing **2**:5-16.

Wang, X., J. Lv, C. Wei, and D. Xie. 2011. Modeling Spatial Pattern of Precipitation with GIS and Multivariate Geostatistical Methods in Chongqing Tobacco Planting Region, China

Computer and Computing Technologies in Agriculture IV. Pages 512-524 *in* D. Li, Y. Liu, and Y. Chen, editors. Springer Boston.

Wenxia, G., C. Xiaoling, C. Xiaobin, Z. Jian, F. Lian, and X. Xiao. 2010. Spatial interpolation of precipitation considering geographic and topographic influences - A case study in the Poyang Lake Watershed, china. Pages 3972-3975 *in* Geoscience and Remote Sensing Symposium (IGARSS), 2010 IEEE International.

Wernli, H., S. Dirren, M. A. Liniger, and M. Zillig. 2002. Dynamical aspects of the life cycle of the winter storm 'Lothar' (24-26 December 1999). Quarterly Journal of the Royal Meteorological Society **128**:405-429.

Wieringa, J. 1973. Gust factors over open water and built-up country. Boundary-Layer Meteorology **3**:424-441.

Wieringa, J. 1986. Roughness-dependent geographical interpolation of surface wind speed averages. Quarterly Journal of the Royal Meteorological Society **112**:867-889.

Wieringa, J. 1997. Representativity problems of wind stations.*in* EU-COST: Data Spatial Distribution in Meteorology and Climatology, Voltera, Italy.

World Meterological Organization. 2008. WMO guide to meteorololgical instruments and methods of observation. Chapter 5: Measurement of surface wind. Chairperson, Publications Board: World Meteorological Organization (WMO), Geneva.

Wu, C., J. Wu, Y. Luo, L. Zhang, and S. D. DeGloria. 2009. Spatial Prediction of Soil Organic Matter Content Using Cokriging with Remotely Sensed Data All rights reserved. No part of this periodical may be reproduced or transmitted in any form or by any means, electronic or mechanical, including photocopying, recording, or any information storage and retrieval system, without permission in writing from the publisher. Permission for printing and for reprinting the material contained herein has been obtained by the publisher. Soil Sci. Soc. Am. J. **73**:1202-1208.

Zlatev, Z., S. E. Middleton, and G. Veres. 2009. Ordinary kriging for on-demand average wind interpolation of in-situ wind sensor data.*in* EWEC 2009, Marseilles.

Zlatev, Z., S. E. Middleton, and G. Veres. 2010. Benchmarking knowledge-assisted kriging for automated spatial interpolation of wind measurements. Pages 1-8 *in* 2010 13th Conference on Information Fusion (FUSION).